

Trunk river and tributary interactions recorded in the Pleistocene–Holocene stratigraphy of the Po Plain (northern Italy)

LUIGI BRUNO* , ALESSANDRO AMOROSI† , STEFANO LUGLI*,
IRENE SAMMARTINO‡ and DANIELA FONTANA*

*Department of Chemical and Geological Sciences, University of Modena and Reggio Emilia, Via Campi 103, Modena, Italy (E-mail: luigi.bruno@unimore.it)

†Department of Biological, Geological and Environmental Sciences, University of Bologna, Via Zamboni 67, Bologna, Italy

‡Geological Consultant, Via Brizio 17/3, Bologna, 40134, Italy

Associate Editor – Christopher Fielding

ABSTRACT

Tributary rivers can contribute significantly to alluvial-plain construction by supplying large volumes of clastic material. Their relation to the main axial river strongly influences sediment deposition and preservation. The Po Plain is fed by the Po River and a dense network of transverse tributaries draining the nearby Alpine and Apennine chains. Stratigraphic, sedimentological, petrographic and geochemical analyses on 38 cores permitted detailed differentiation of Po and Apennine sedimentary units. Po River deposits are vertically stacked channel-belt sand bodies with high contents of quartz–feldspar and metamorphic rock fragments, combined with high chromium levels. These sand bodies, 20 to 30 km wide, are replaced southward by finer-grained deposits that represent the distal Apennine tributary-rivers system. Apennine sands, confined in narrow ribbons, show lower quartz–feldspar contents, abundant sedimentary lithics and lower chromium levels. In the last 870 kyr, the boundary between the Po and the Apennine sediment delivery systems shifted along a north–south axis in response to distinct controlling factors. A 20 km northward shift of the Po channel belt, possibly related to a tectonic event, is recorded across a regional unconformity dating to the Marine Isotope Stage 12/11 transition. High sediment supply rates during glacial-lowstand periods widened the Po channel belt southward towards the Apennine domain for a few kilometres. The Last Glacial Maximum channel-belt sand body, 30 km wide and 40 m thick, progressively narrowed northward after the glacial culmination. During the Holocene, channel patterns became avulsive and distributive. Narrow channel belts (<3 km) formed along the Po River branches, and abundant swamp and poorly drained-floodplain muds were preserved in interfluvial areas. Activation and deactivation of the Po branches resulted in sharp narrowing and widening of the area available for Apennine-rivers sedimentation. This work provides insights into tributary-trunk river relations which control grain-size distribution and compositional characters of subsurface deposits.

Keywords Pleistocene–Holocene, Po Plain, sediment provenance, subsurface stratigraphy, tributaries, trunk river.

INTRODUCTION

Continental successions are valuable archives of information on past environmental changes that occurred in response to distinct forcing factors. Vertical changes in fluvial-channel stacking patterns have been observed in ancient and Quaternary alluvial successions worldwide (Cleveland *et al.*, 2007; Labourdette & Jones, 2007; Kasse *et al.*, 2010; Blum *et al.*, 2013; Mancini *et al.*, 2013; Newell *et al.*, 2015; Campo *et al.*, 2016). The relative influence of distinct controlling factors on these variations has been discussed in several studies (Schumm, 1993; Martinsen *et al.*, 1999; Blum & Törnqvist, 2000). Glacio-eustasy has been regarded as the main factor controlling alluvial sedimentation after the Early–Middle Pleistocene transition, *ca* 900 kyr BP (Busschers *et al.*, 2005; Gibling *et al.*, 2005; Blum & Aslan, 2006). In these studies, stratal architecture was compared with a well-known climatic and eustatic history reconstructed through independent global and local proxies (e.g. Dansgaard *et al.*, 1993; Waelbroeck *et al.*, 2002). Late Quaternary investigations are also advantaged by the detailed knowledge of the drainage system, which permits reliable reconstructions of the source-to-sink patterns of sediment dispersal. The mutual relations between the trunk river and its tributaries have been explored in previous studies, which addressed: (i) the differences in composition between tributaries and trunk-river sediments (Sinha *et al.*, 2009; Garzanti *et al.*, 2011; Tentori *et al.*, 2016, 2018); (ii) the geomorphic response of tributaries to axial river incision (Leeder & Stewart, 1996; Posamentier, 1998, 2001; Posamentier & Allen, 1999; Green, 2009); (iii) wetland formation due to tributary fan progradation in trunk river valleys (McCarthy *et al.*, 2011); (iv) erosion of the toes of tributary fans by trunk-river lateral migration (Bishop, 1995; Larson *et al.*, 2015); (v) tributary–trunk river interactions due to hydrological changes over a few decades (Meade & Moody, 2010; Xu, 2016). Kvale & Archer (2007) and Vis *et al.* (2008) described the sedimentological characteristics and internal architecture of tributary incised valleys. The preservation potential of tributary networks has been discussed in several papers (Fielding *et al.*, 2012, and references therein).

Through the analysis of the stratigraphic relations between Po and Apennine river deposits, this work aims at evaluating: (i) the extent to which tributary rivers may contribute to

sediment accumulation in alluvial plains; and (ii) how sedimentological and compositional characters of the preserved sediments are influenced by the interactions between the trunk river and its tributaries through time.

The Pleistocene–Holocene stratigraphy of the Po Basin was reconstructed in a 4000 km² wide sector of the Po Plain, *ca* 70 km away from the modern coastline, with the aims of examining patterns of sediment dispersal and depicting major shifts in sediment provenance between the Po–Alpine and the Apennine river systems. For this purpose, 38 cores were analysed and correlated along six stratigraphic cross-sections, together with 300 stratigraphic data (published core descriptions, piezocone penetration tests and well logs). A 450 m deep cross-section explored the stratigraphy of the Po Supersynthem, an unconformity-bounded unit dated to the last 870 kyr. Five cross-sections focused on the Late Pleistocene–Holocene depositional architecture (last 50 kyr). This time window, encompassing the last glacial period and the present interglacial, offers the opportunity to study the response of the trunk river and of its tributaries to high-magnitude climate and eustatic changes.

GEOLOGICAL SETTING

Structural setting and subsurface stratigraphy

The Po Plain represents the foredeep of the Southern Alps and of the Northern Apennines, filled with Pliocene–Quaternary sediments (Fig. 1A). The Alpine and Apennine thrust belts developed in response to the convergence between the African and European plates, starting in the Cretaceous (Carminati & Doglioni, 2012) and still progressing at the rate of 3 to 8 mm/yr (Devoti *et al.*, 2011).

The Northern Apennines developed since the Neogene on the hanging wall of a west-directed subduction zone (Livani *et al.*, 2018, and references therein). The most external portion of the Northern Apennine accretionary wedge is buried beneath the Po Plain (Fig. 1B) and is composed of three arcuate systems of thrust-related folds (Fantoni & Franciosi, 2010; Turrini *et al.*, 2014). From west to east: the Monferrato, Emilia and Ferrara–Romagna folds. The Ferrara–Romagna folds have been tectonically active since the Early Pliocene (Toscani *et al.*, 2009; Boccaletti *et al.*, 2011; DISS Working Group, 2018).

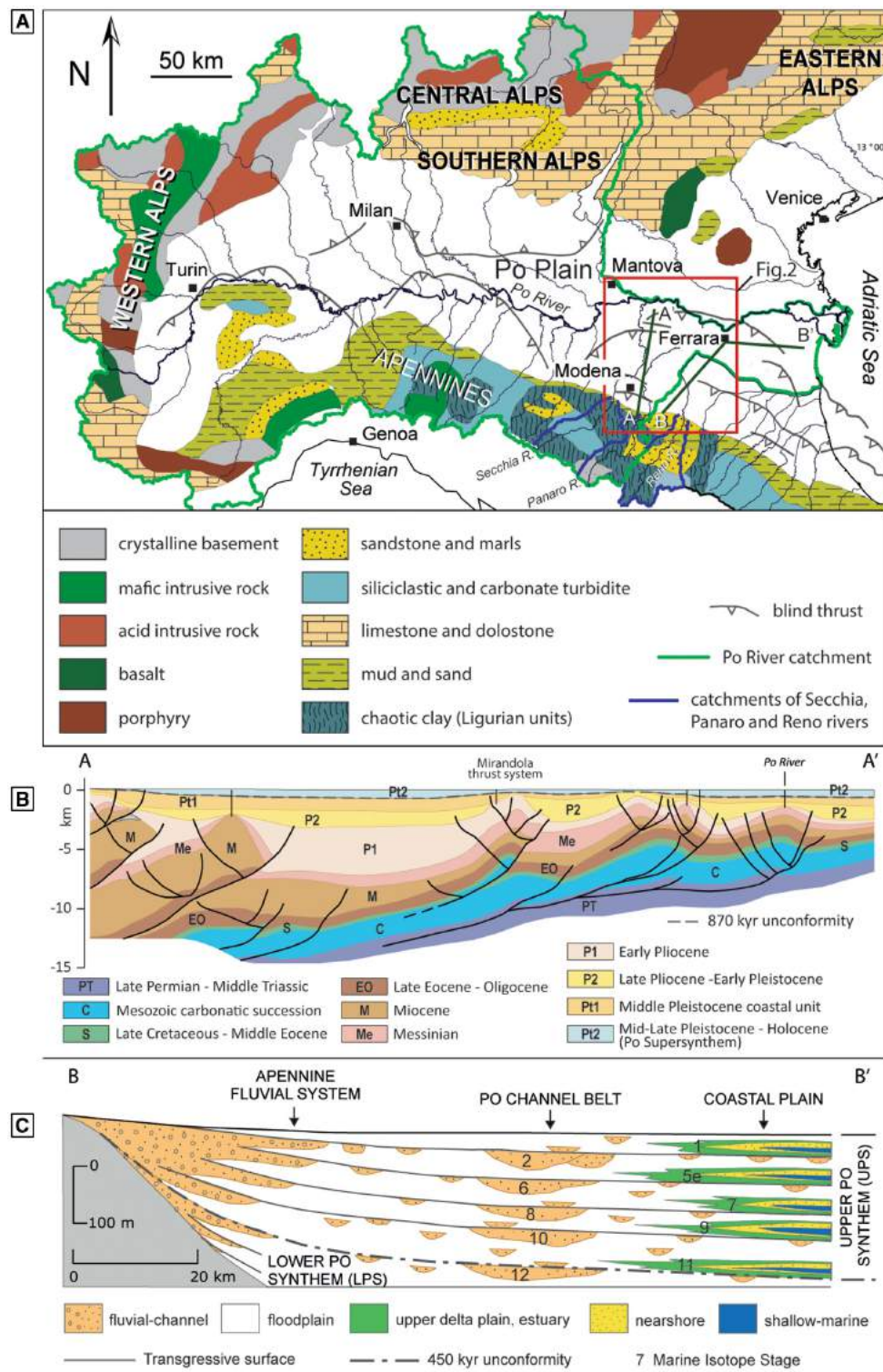


Fig. 1. (A) Geological map showing the main rock units cropping out in the drainage basins of the Po, Secchia, Panaro and Reno rivers. The projection of the main thrusts buried beneath the Po Plain is also outlined. (B) Interpreted seismic profile showing the Po Basin fill (units P1 to Pt2) overlying the Permian to Miocene substrata, intensely deformed by north-verging Apennine thrusts. (C) Stratigraphic architecture of the Po Supersynthem (Pt2 in Fig. 1B) along an idealized profile from the Apennine margin to the modern coastal plain (modified after Amorosi *et al.*, 2017a).

Particularly, some faults of the Ferrara–Romagna Arc (i.e. Mirandola thrust system) were activated during the 2012 Emilia earthquake (Bonini *et al.*, 2014) with fault plane solutions indicating dominantly compressional mechanisms (Pondrelli *et al.*, 2012; Scognamiglio *et al.*, 2012).

The thickness of the Plio-Quaternary Po Basin fill ranges from 6 to 8 km in the depocentres to *ca* 100 m at the top of the buried anticlines (Amadori *et al.*, 2019). The basin fill comprises: (i) Zanclean–Calabrian turbidites (P1 and P2 in Fig. 1B), syntectonically deposited in isolated piggy-back basins and in the foreland prism (Ghielmi *et al.*, 2013); and (ii) Middle Pleistocene–Holocene coastal (Pt1) and continental units (Pt2, Fig. 1B). Unit Pt2 (Po Supersynthem of Amorosi *et al.*, 2008) is dated to the last 870 kyr BP (Muttoni *et al.*, 2003, 2011; Scardia *et al.*, 2006; Gunderson *et al.*, 2014) and is subdivided into two depositional sequences (Lower and Upper Po Synthem, Fig. 1C) by a regional unconformity dated to 450 kyr BP (Geomol Team, 2015; Martelli *et al.*, 2017).

The Upper Po Synthem (UPS in Fig. 1C) is partitioned into five smaller-scale depositional successions (transgressive–regressive cycles of Amorosi *et al.*, 2004; Fig. 1C). Beneath the modern coastal plain each succession consists of shallow-marine and coastal sediment bodies overlain by alluvial deposits (Fig. 1C). Close to the Apennine margin and beneath the Po River, the landward equivalents of these transgressive–regressive successions are composed of mud-dominated overbank strata that transition upward to regionally extensive fluvial channel bodies. Pollen series from 150 m deep cores (Amorosi *et al.*, 2004, 2008) and electron spin resonance dates (Ferranti *et al.*, 2006) document that shallow-marine coastal bodies were deposited during late transgression and highstand of interglacial periods, whereas laterally extensive channel-belt sand bodies accumulated during forced regression and lowstand of glacial periods (Campo *et al.*, 2020).

Surface geology of the drainage system

The Po River originates in the Western Alps and flows easterly for 652 km (Fig. 1A). It receives water and sediments from 141 tributaries, which drain a cumulative area of about 75 000 km². The western part of the Po drainage basin, including large sectors of the Western and Central Alps and of the western Apennines, is

characterized by extensive outcrops of crystalline–metamorphic and ophiolite complexes (Fig. 1A). In contrast, Mesozoic carbonate rocks are extensively exposed in the Southern and Eastern Alps (South-Alpine units in Fig. 1A).

The southern part of the study area is fed by three major Apennine rivers: Secchia, Panaro and Reno (Fig. 1A). These rivers have remarkably smaller catchment areas (<2300 km²), mainly composed of Cretaceous tectonically deformed clays with carbonate blocks (Ligurian Units in Fig. 1A; Remitti *et al.*, 2011) and of Palaeocene to Neogene coastal-marine sandstones and marls (Epiligurian Units in Fig. 1A; Ricci Lucchi, 1987). Pliocene shallow-marine clays and subordinate Pleistocene coastal sands crop out at the Apennine margin (Post-Evaporitic Units in Fig. 1A, Ricci Lucchi *et al.*, 1982). The Secchia and Panaro rivers are tributaries of the Po River, whereas the Reno River, which flows nowadays into the Adriatic Sea, has been a tributary of the Po River in the past centuries, as highlighted by historical maps (available online at <http://geoportale.regione.emilia-romagna.it>).

METHODS

The stratigraphic dataset

This study relies upon sedimentological, petrographic and geochemical analyses of 38 cores (locations shown in Fig. 2). Core length, generally <50 m, permitted the detailed investigation of Late Pleistocene and Holocene units (last 50 kyr). Only cores MIR and MED, 127 m and 111 m long, respectively, penetrated the entire Po Supersynthem (last 870 kyr). Cores were retrieved with a rotary-wash drilling method, which allowed high percentages (>90%) of sample recovery for fine-grained material. This technique, however, does not permit the preservation of sedimentary structures in sands. Cores were described in terms of lithology, grain-size, colour, consistency and accessory material (macrofossils, vegetal remains, peat and carbonate concretions). *In situ* tests include pocket-penetrometer measurements and estimates of the CaCO₃ content through reaction to HCl. Additional facies analysis was carried out in a 5 m long and 3 m deep trench (San Carlo trench, Fig. 2), where sediment deposited by a palaeo-Reno River, active during the 18th Century, have been exposed (Caputo *et al.*, 2012).

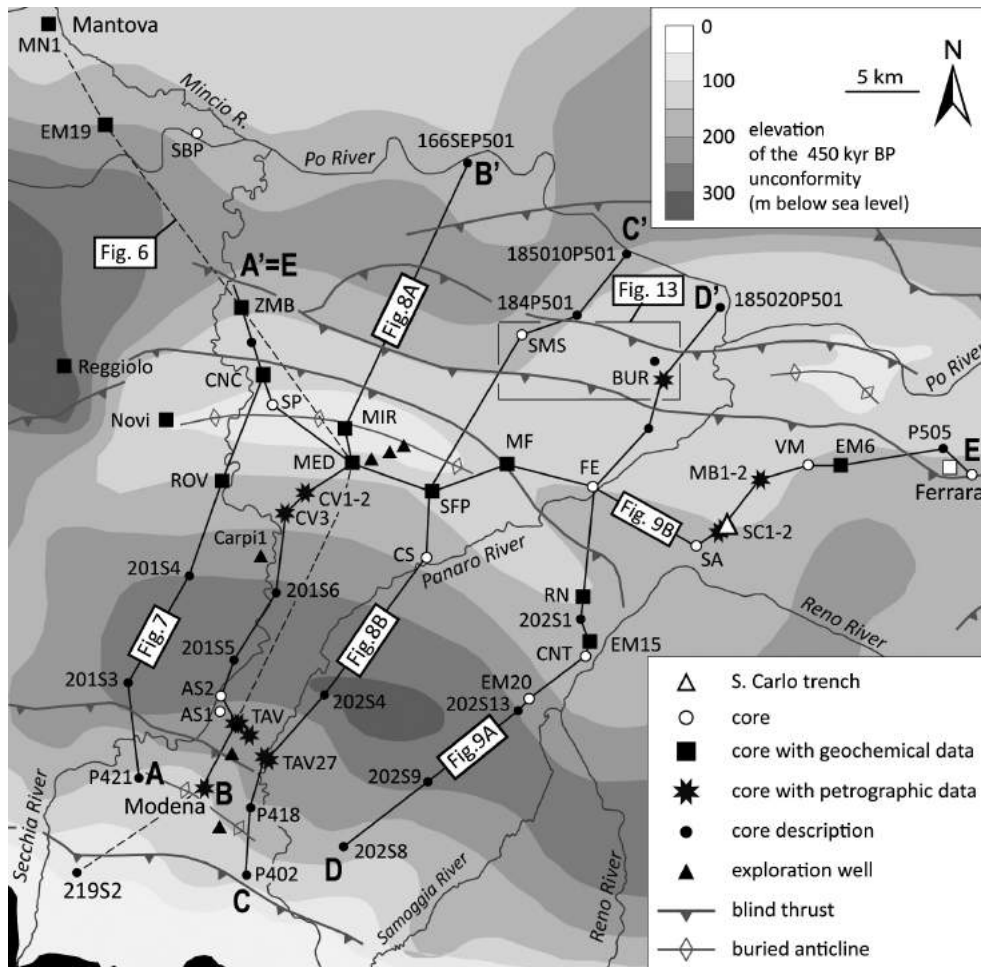


Fig. 2. Study area with location of the analyzed cores, the sampling sites for petrographic and geochemical analyses, and the trace of the stratigraphic cross-sections of Figs 6 to 9. The elevation (metres below modern sea level) of the 450 kyr unconformity and the projection of buried tectonic structures is also shown (modified after Martelli *et al.*, 2017).

The stratigraphic dataset also includes 40 core descriptions, 145 well logs (logged lithological sections and downhole wireline logs) and 122 piezocone penetration tests (CPTUs). Core descriptions refer to boreholes drilled for the Geological Mapping of Italy to scale 1 : 50,000 project (depth <180 m) and provide high-quality information on lithology, colour, consistency, reaction to 10% HCl, pocket-penetrometer measurements, and radiocarbon dates. Basic lithological descriptions (i.e. sand versus mud) deriving from the analysis of well cuttings were used to reconstruct the geometry of fluvial-channel bodies at depths between 50 m and 500 m. Lithological information (cuttings), resistivity logs and palaeontological data from six exploration wells (depth >500 m) were used as

anchor points to track the base of the Po Supersynthem (see *Stratigraphy of the Po Supersynthem* section). Piezocone tests were interpreted based on Amorosi *et al.* (2017a) after calibration with nearby cores (see *Facies association* section).

Sediment provenance analysis

Petrographic and geochemical analyses of samples collected at depth <50 m allowed the recognition of the Po versus Apennine provenance of Late Pleistocene and Holocene sediments in the uppermost two cycles of unit UPS (Fig. 1C). Sediment provenance interpretations also relied upon petrographic data from Lugli *et al.* (2004; TAV cores) and Fontana *et al.* (2015, 2019; cores

SC1-2 and MB1-2), and geochemical data from Amorosi *et al.* (2016; cores CNC, ROV and ZMB) and Bruno *et al.* (2018; cores EM19, MN1 and Novi). Information on the sediment provenance of older units derive from Amorosi & Sammartino, 2018, cores MIR and MED) and from the Sheets 181, 202 and 203 of the Geological Map of Italy to scale 1 : 50.000.

Petrographic analyses were carried out on 19 sand samples collected from four cores (CV1, CV2, CV3 and Modena). For each sample, the bulk sand was used for qualitative petrographic observations, whereas point counting was carried out on the fine sand fraction (0.125–0.250 mm) separated by dry sieving. Modal analysis was performed according to the Gazzi-Dickinson method designed to minimize the dependence of the analysis on the grain size (Zuffa, 1985). At least 300 grains were point counted for each section. Components not related to the original sand composition, such as authigenic carbonate nodules and other particles originated from soil erosion, and organic matter and penecontemporaneous shell fragments were excluded from final calculations. The modal analyses were compared with detrital modes from modern rivers: Po (four samples, this work), Reno (four samples, Fontana *et al.*, 2015), Secchia, Panaro and its minor tributaries (42 samples, Lugli *et al.*, 2004, 2007).

Geochemical analyses were performed on 60 sand-to-clay samples collected from 10 cores (CNC, EM6, EM15, MF, MED, MIR, ZMB, RN, ROV and SFP, Fig. 2). Sixty-eight additional near-surface (<1.5 m) samples portrayed on the *Pedogeochemical Map of Regione Emilia-Romagna* (Amorosi *et al.*, 2014) were used as reference for sediment-provenance characterization of subsurface deposits. All samples were oven-dried at 50°C, powdered and homogenized in an agate mortar and analyzed by X-ray fluorescence (XRF) spectrometry for major element oxides, loss on ignition, and trace metals using a Philips PW 1480 spectrometer (Koninklijke Philips N.V., Amsterdam, The Netherlands). The matrix correction methods reported in Leoni *et al.* (1986) were followed. Certified reference material, including samples BR, BCR-1, W1, TB, NIM-P, DR-N, KH and AGV-1 (Govindarajiu, 1989) was also analyzed. The estimated precision and accuracy for trace-element determinations was 5%. For elements with concentrations <10 ppm, the accuracy was 10%.

Stratigraphic correlation and absolute chronology

The stratigraphy of the Po Supersynthem (last 870 kyr) was investigated down to 500 m depth, along a south–north oriented, 75-km long cross-section between the Apennine foothills and the town of Mantova (dashed line from core 219S2 to MN1 in Fig. 2). Nineteen core logs, 62 water-well logs and six exploration well-logs were correlated, with a mean distance between the core locations of 1.1 km. The Late Pleistocene–Holocene depositional architecture (last 50 kyr) was investigated along four south–north oriented cross-sections (AA' to DD', Fig. 2) and a west–east oriented transect (EE' in Fig. 2). Sections AA' to EE' are 50 to 80 m thick and 40 to 60 km long. The mean distance between the core locations is *ca* 1.0 km.

Stratigraphic correlations were based on geometric criteria, chronologically constrained by: (i) a pollen series from the 114 m long core MN1 (Amorosi *et al.*, 2008); (ii) 60 radiocarbon dates from Vittori & Ventura (1995); Amorosi *et al.* (2016, 2017a), Campo *et al.* (2016), Bruno *et al.* (2018) and the Geological Map of Italy (sheets 201, 202, 220; see Data S1); and (iii) archaeological reports, collected and summarized in Caldarelli & Malnati (2003) and Biancardi (2013), which provide chronological information for Late Holocene deposits. Additionally, 25 samples of sediment, peat, wood and vegetal remains were dated at KIGAM (Republic of Korea), Ion Beam Physics (ETH, Switzerland), CIRCE (Italy) and ENEA (Italy) laboratories. Radiocarbon ages were calibrated using OxCal 4.4 (Bronk Ramsey & Lee, 2013) with the IntCal 20 curve (Reimer *et al.*, 2020).

RESULTS

Facies associations

Five facies associations were identified in the analysed cores and in the S. Carlo trench (location shown in Fig. 2). These are characterized as follows.

Fluvial channel (FC)

Description. This facies association is composed of 3 to 20 m thick gravel and sand bodies with erosional or sharp base and fining-upward (FU) grain-size trend (from coarse to fine sand). Gravel bodies, observed only in the southern

cores (Modena and TAV, Fig. 2), are composed of sub-rounded, heterolithic cobbles and pebbles in a sandy or silty matrix. In northern cores, grey (2.5YR 7/1) coarse sands form >8 m thick sediment bodies, with occasional pebble layers at the base (Fig. 3B). In cores MIR and MED, at depths >90 m, sands are grey-peach (5YR 8/2), with heterolithic pebbles and cobbles (mainly dolostone and porphyry with diameter <5 cm). In core sands sedimentary structures are not preserved. High-angle planar and trough cross-stratification has been observed in yellowish sands (2.5Y 8/2) of the San Carlo trench (Fig. 3A). Body fossils are absent and wood fragments are seldom encountered. In CPTUs adjacent to the analysed cores, tip-resistance values (q_c) are in the range of 3 to 20 MPa, with an overall decreasing upward trend. Pore pressure (u) values are negative.

Interpretation. Based on the lithology and grain-size, this facies association is interpreted as deposited in a high-energy environment. Sharp or erosional bases, basal pebble-layers, FU

grain-size trends, traction structures and scattered wood fragments are common features of fluvial-channel deposits (Allen, 1963). Gravels observed in southern cores, close to the Apennine foothills, are interpreted as braided-river deposits (Miall, 1985, 1996; Bridge, 1993). The lack of preserved sedimentary structures in cores does not permit a detailed facies attribution. High q_c values are typical of coarse-grained material (Schmertmann, 1969). Negative u values reflect rapid dissipation of the excess pore pressure generated by the penetration of the cone (Campanella *et al.*, 1982). The presence of dolostones and porphyries in northern cores at depth >90 m suggests provenance from the Southern Alps (Amorosi & Sammartino, 2018).

Crevasse and levée (CL)

Description. This facies association includes <3 m thick sediment bodies, laterally or vertically associated with FC deposits, composed of: (i) fine to silty sand with FU trend; (ii) coarsening-upward (CU) silty to fine sand; and (iii) sand–mud alternations at centimetre to

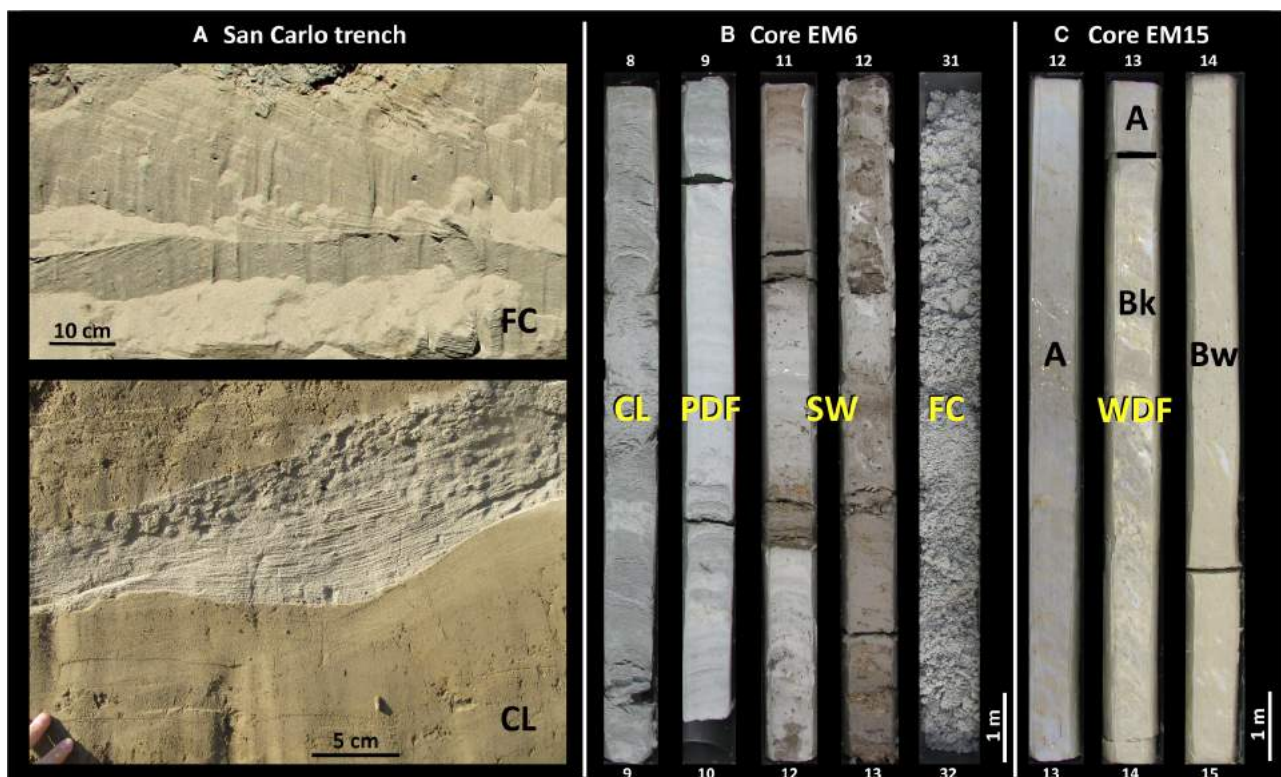


Fig. 3. Representative photographs of facies associations observed in the S. Carlo trench (A) and in cores EM 6 (B) and EM15 (C). See Fig. 2 for location. FC: fluvial channel; CL: crevasse and levée; PDF: poorly drained floodplain; SW: swamp; WDF: well-drained floodplain. For pedological horizons A, Bk and Bw, see text and Table 1.

decimetre scales. Colour is grey (7.5YR 8/1) or beige (10YR 8/2). Body fossils are absent. FU sand bodies have small lateral extent (<20 m), concave-up base and flat upper surfaces. Cross-stratification was commonly observed in outcrop and wood fragments were encountered locally. CU sand bodies, a few tens of metres wide, have nearly tabular shape with faint convex-up upper boundary. Sub-horizontal laminae due to thickening-upward coarser strata are observed. In sand–mud intercalations, mud strata are structureless and bioturbated, with sparse carbonate concretions and root traces. Sandy horizons have sharp or erosional lower boundary and are laminated or cross-bedded (*CL* in Fig 3A). Sand–mud couplets gently slope towards adjacent floodplain muds. Thickness and sand–mud ratio decrease downslope. In CPTU tests, q_c is <10 MPa, whereas $u < u_o$ (static equilibrium pore pressure).

Interpretation. Sedimentological features and the close association with the fluvial-channel bodies allow interpretation of these deposits as channel-related facies. Particularly, sand bodies with erosive base and internal FU trend are interpreted as crevasse channels (Singh, 1972), whereas sheet-like sand bodies with CU trend are referable to crevasse splays. Sand–mud alternations grading into adjacent floodplain muds could represent channel levées (Alexander & Prior, 1971), formed by proximal over-bank deposition. Bioturbation and root traces testify to incipient pedogenesis between successive overflow events. Sparse carbonate concretions likely reflect local groundwater-table fluctuations.

Well-drained floodplain (WDF). Description. This facies association is composed of thick (>10 m), subtly varying successions of hardened clayey silt and silty clay. Palaeosols were recognized at discrete stratigraphic intervals, marked by the presence of diagnostic horizons (A, Bk and Bw, Fig. 3C and Table 1). A horizons, up to 1 m thick, are dark brown (7.5YR 6/2) and show no or faint reaction to HCl. Bk horizons are typified by abundant carbonate concretions in the form of coalescent nodules and coatings. Bw horizons exhibit faint mottles of Fe and Mn oxihydroxides. The observed palaeosols show A–Bk–Bw, A–Bk or A–Bw profiles. Pocket penetrometer values are 2 to 3 kg/cm², with higher values (>3 kg/cm²) in Bk horizons. Fossils are absent. In CPTUs, q_c and f_s (lateral friction) are

in the range of 1 to 3 MPa and 50 to 150 kPa, respectively. Pore pressure is generally greater than u_o .

Interpretation. The dominance of fine-grained material suggests deposition in a low-energy interfluvial environment (Collinson, 1978). Palaeosols with A–Bk or A–Bk–Bw profiles have been interpreted as Inceptisols (Soil Survey Staff, 1999; Buol *et al.*, 2011); palaeosols with A–Bw profiles as Entisols (Soil Survey Staff, 1999; Kraus, 1999). The mobilization of carbonates and their transfer into the soil profile suggest low groundwater table during exposure (well-drained floodplain). Unlike deeply weathered reddish soils (McCarthy & Flint, 1998; Abels *et al.*, 2013; Kraus *et al.*, 2015), these palaeosols show evidence of only incipient pedogenesis (Amorosi *et al.*, 2014, 2017a). In Inceptisols, the characteristics of secondary calcite (evolutionary stages 2 and 3 of Gile *et al.*, 1981; Machette, 1985) are consistent with exposure periods of a few thousand years (Bruno *et al.*, 2020a). Entisols likely result from exposure periods of a few hundred years (Kraus, 1999). Low q_c and $u > u_o$ are typical of fine-grained material (Robertson *et al.*, 1986). Relatively high f_s is referable to pedogenic processes (Amorosi *et al.*, 2017a).

Poorly drained floodplain (PDF)

Description. This facies association is composed of soft, light-grey (2.5YR 8/1) clayey silt and silty clay, *ca* 3 m thick, with faint horizontal lamination (Fig. 3B). Isolated carbonate concretions are seldom encountered. Fossils and oxides–hydroxides were not observed. Pocket penetrometer values range between 1 and 2 kg/cm². In CPTUs, q_c and f_s are in the range of 0.8 to 1.2 MPa and 20 to 50 kPa, respectively. Pore pressure is greater than u_o . This facies association is commonly sandwiched between well-drained floodplain and swamp deposits.

Interpretation. This facies association has been interpreted as deposited in a poorly drained floodplain, with water table fluctuating close to the topographic surface. This interpretation is consistent with its stratigraphic position between well-drained floodplain and swamp deposits. A relatively high level of the groundwater table likely prevented eluviation–illuviation and oxidation. The formation of sparse and isolated carbonate concretions is likely due to water-table fluctuations.

Table 1. Diagnostic features of palaeosol horizons.

Palaeosol	Horizon	Thickness (cm)	Colour	Reaction to HCl	Carbonate concretions	Redoximorphic features	Pocket penetrometer (kg/cm ²)
Inceptisol	A	30–100	Dark grey, brown (7.5YR 6/2)	Absent	Rare isolated nodules (diameter <2 mm)	Faint mottles of Fe and Mn oxides	2.0–3.0
	Bk	30–120	Beige (10YR 8/2)	Strong	Abundant coalescent nodules (diameter: 2–5 mm), filaments and coatings	Faint mottles of Fe and Mn oxides	>3.0
	Bw	0–150	Grey (7.5YR 8/1) with orange (7.5YR 7/4) mottles	Faint or medium	Rare isolated nodules (diameter <2 mm)	Mottles of Fe and Mn oxides	2.0–3.0
Entisol	A	10–30	Dark grey (7.5YR 6/2)	Faint	Rare isolated nodules (diameter <2 mm)	/	2.0–2.5
	Bw	30–100	Grey (7.5YR 8/1) with orange (7.5YR 7/4) mottles	Faint or medium	Rare isolated nodules (diameter <2 mm)	Faint mottles of Fe and Mn oxides	2.0–2.8

Swamp (SW)

Description. This facies association is composed of soft, light grey (7.5YR 8/1) silty clay, 3 to 5 m thick, with abundant undecomposed vegetal remains and peat (Fig 3C). Pocket penetrometer values are <1 kg/cm². Freshwater gastropods were seldom encountered. Oxides and carbonate concretions were not observed. Low q_c (<0.8 MPa) and f_s (<30 kPa) typify this facies association. Pore pressure is $>u_0$.

Interpretation. The dominance of fine-grained material suggests deposition in a distal low-energy environment. Light grey colour of muds reflects poor degradation of organic material. The preservation of undecomposed plant material and the lack of oxides and secondary carbonates, together with low q_c and f_s values, suggest deposition in an environment with persistently high water table (for example, swamp; Diessel, 1992; Richardson & Vepraskas, 2001; Stolt & Rabenhorst, 2011).

Po versus Apennine sediment provenance

The Po Plain is a multi-sourced system, where Alpine and Apennine lithostratigraphic units

display distinctly different compositional signatures. Provenance of Late Pleistocene and Holocene sediments has been assessed by comparing modal compositions of detrital grains and geochemistry of the cored samples with those of modern sediments from the Secchia, Panaro, Reno and Po rivers (Figs 4 and 5).

Sand petrography

Modern sands from the Apennine rivers (Secchia, Reno, Panaro and minor streams, Fig. 4A) have an overall litharenitic composition. The lithic association includes sedimentary siliciclastic grains (siltstones and shales) and carbonate lithics (largely micritic limestones and calcite spars). Shale grains are consolidated, well-rounded, with iso-orientation of the clay minerals, revealing their detrital origin. Modern Po River sands in the study area are distinguishable from Apennine sands by their significantly higher content of quartz–feldspar (Fig. 4A), coarse-grained metamorphic rock fragments, micas and heavy minerals. Sedimentary lithics are subordinate and consist of carbonate, with minor siltstone and shale grains. Carbonate lithics are more abundant downstream of the confluence with the

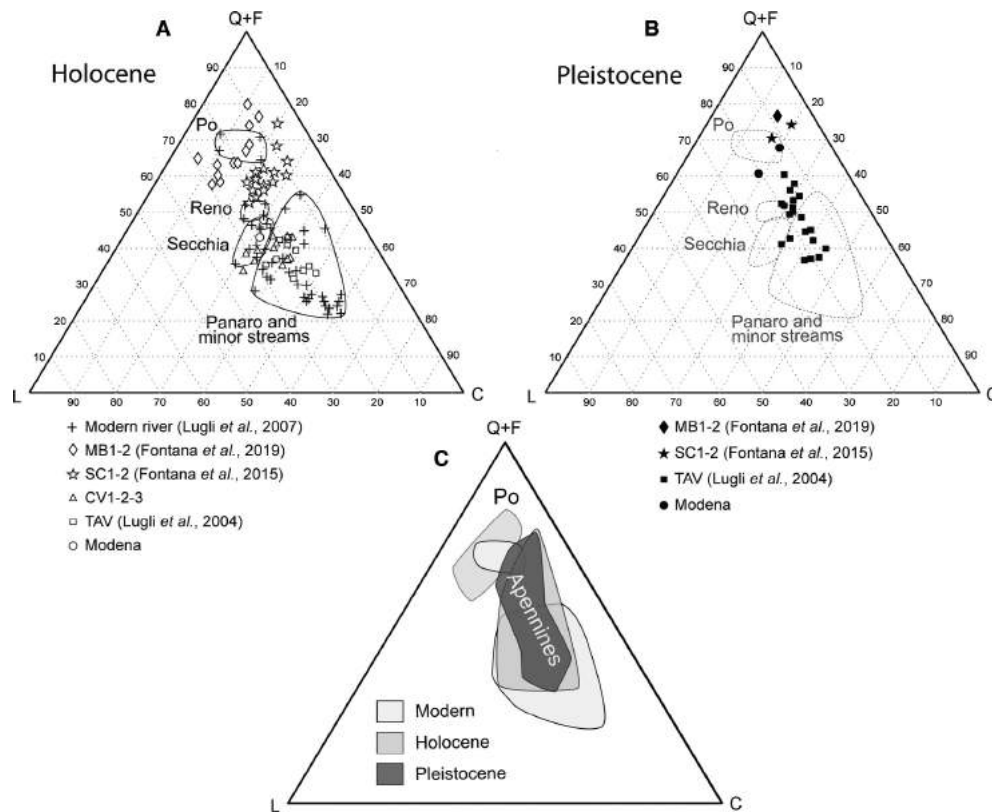


Fig. 4. Ternary diagram showing the composition of modern, Holocene (A) and Pleistocene (B) sands from modern rivers and cores. The compositional fields back to the Pleistocene are shown in (C) ('Q': quartz; 'F': feldspars; 'L': siliciclastic rock fragments; 'C': carbonate rock fragments).

Panaro River. Serpentinite and volcanic grains are minor components.

The composition of Holocene sands is variable. Sands from southern cores (Modena, TAV, CV1, CV2 and CV3, location in Fig. 2) are similar to those of the modern Secchia and Panaro rivers. By contrast, sands from the northern cores (MB1 and MB2) show a quartz–feldspar-rich composition similar to the modern Po River. Sands of the 18th Century Reno River (S. Carlo trench and cores SC1-2) have markedly lower contents of lithics, in particular shale and carbonate grains, compared to the modern Reno compositional field (Fig. 4A).

Late Pleistocene samples from cores Modena, TAV, CV1, CV2 and CV3 are within the compositional fields of modern Apennine rivers, but show an overall lower amount of sedimentary lithics and higher quartz and feldspar contents (Fig. 4B). This enrichment is particularly significant for cores Modena, SC1 and SC2, which partly overlap the compositional field of the modern Po River. Samples from the northernmost cores

(MB1 and MB2) yielded the highest quartz and feldspar contents. Sand grains appear relatively unaffected by alteration and corrosion.

Petrographic data reflect substantial differences in extent and lithology of the drainage catchments between the Po and Apennine rivers. The major trunk river (Po) carries detritus well-mixed from wider sectors of the Alpine and Apennine orogens over a longer distance (Fig. 1A). As a result, the Po sand is mainly composed of quartz-rich and feldspar-rich grains and metamorphic rock fragments. On the contrary, Apennine rivers have relatively smaller catchments and supply detritus mainly from sedimentary strata. In particular, the Ligurian units represent the primary source of shales and carbonates to the river network. The overall higher quartz and feldspar contents locally observed in Apennine Pleistocene samples seem to be primarily controlled by weathering conditions during the last glacial stage. Denudation, erosion and accelerated transport were probably responsible for the disintegration and microfracturing of lithic sedimentary

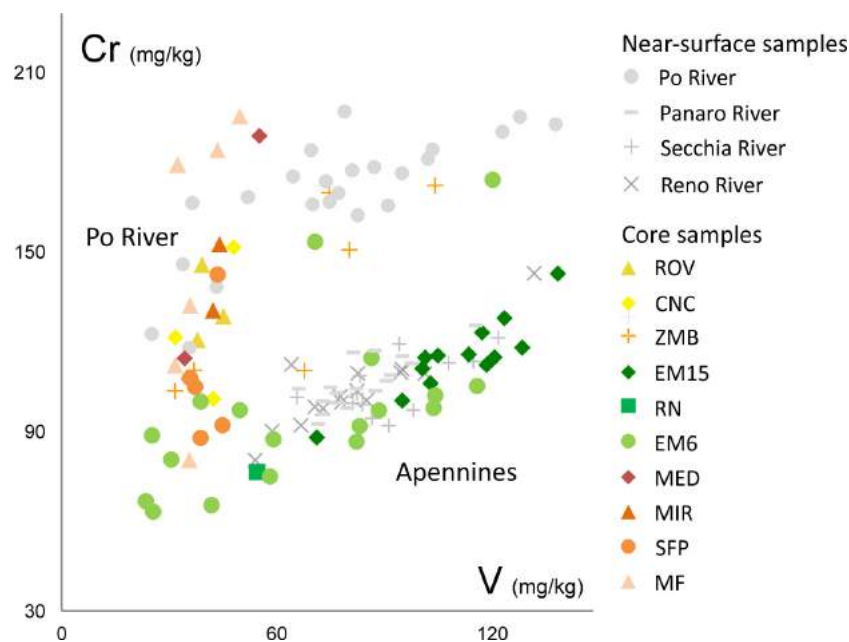


Fig. 5. Scatterplots of V versus Cr from 60 core samples (in colour) showing the Po, Apennine and mixed sediment compositions. Sixty-eight reference samples from Po versus Apennine modern deposits are in grey.

grains, thus promoting an indirect increase of quartz and feldspar in sands (Lugli *et al.*, 2007).

Sediment geochemistry

The distinctive difference in drainage-basin bedrock composition between the Po River catchment and Apennine (Secchia, Panaro and Reno) river watersheds (Fig. 1) is strongly reflected by trace-element geochemistry. Weathering of peridotite, gabbro, basalt and ophiolitic rocks, cropping out extensively in the Western Alps and at the north-western tip of the Apennines (Fig. 1), delivers large volumes of Cr-rich and Ni-rich detritus to the Po River system (Amorosi *et al.*, 2014). A typical element ratio that was tested successfully in modern Po Plain sediments for the discrimination of Po River versus Apennine rivers provenance composition is Cr/V, irrespective of sandy versus muddy lithologies (Amorosi & Sammartino, 2007; Amorosi *et al.*, 2014). An equally effective normalization factor of geochemical data that has been used to emphasize the role of parent-rock composition is the Cr/Al₂O₃ ratio (Greggio *et al.*, 2018). The Cr/V ratio, adopted in this paper, has been commonly used as a key index for sediment provenance from mafic and ultramafic rocks (Garver *et al.*, 1996; Lužar-Oberiter *et al.*, 2009). In the Po Plain, this ratio exhibits distinctly higher values along the

Po River, whereas very low levels are invariably recorded in near-surface samples of its Apennine tributaries (Secchia, Panaro and Reno rivers in Fig. 5).

In the study area, Late Pleistocene and Holocene samples from the southernmost cores (EM15 and RN in Fig. 2) exhibit distinctively low Cr/V levels that plot invariably into the compositional fields of Apennine river sediments, across all grain sizes (Fig. 5). In contrast, samples from cores ZMB, CNC, ROV, MED, MIR and MF, despite being located up to 25 km south of the modern Po River (Fig. 2), show a characteristic Po River affinity, with consistently higher Cr/V values (Fig. 5). Core samples from EM6 and SFP plot considerably off of this general trend and display mixed (Po and Apennines) geochemical signatures (Fig. 5).

The spatial distribution of individual core samples and their relation to stratigraphic architecture is shown and discussed in the next sections.

Stratigraphy of the Po Supersystem

Middle Pleistocene stratigraphy

Above the folded and faulted Plio-Pleistocene substratum, the Po Supersystem has variable

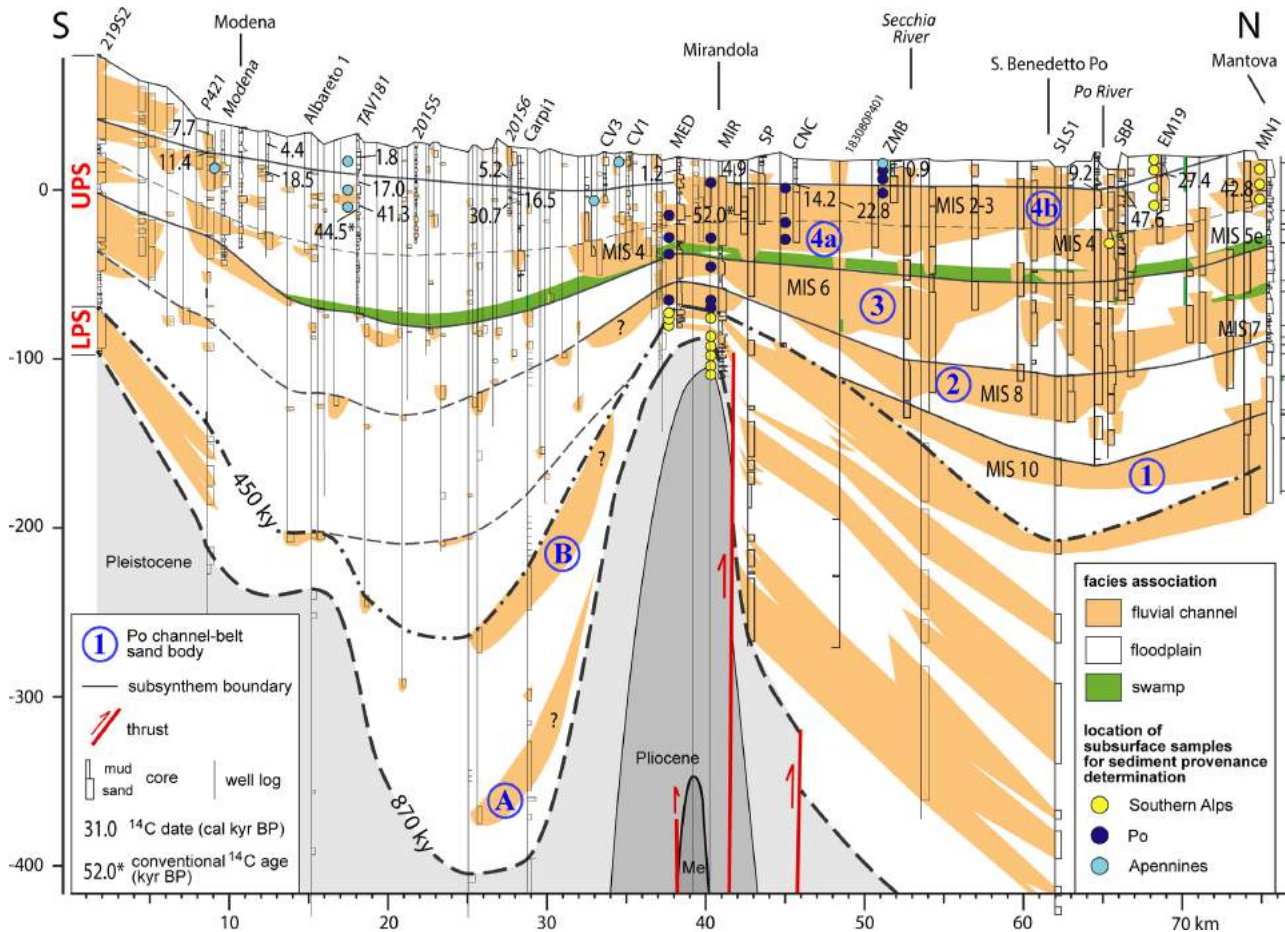


Fig. 6. Stratigraphy of the Po Supersystem along a north–south-oriented profile from the Apennine margin to Mantova. Location in Fig. 2.

thickness, from *ca* 100 m close to the Apennine margin and above the culmination of the Mirandola Anticline, to *ca* 400 m in the depocentres. The base of the Po Supersystem, observed in cores 219S2 and MIR and in deep exploration wells, is characterized by the upward transition from coastal to continental deposits (Fig. 6).

In the northern sector, laterally extensive fluvial-channel sand bodies alternate with mud-prone strata (Fig. 6). In core MN1, the upward transition from mud to sand is marked by a decline in pollen from warmth-loving species (i.e. broad-leaved trees), with a parallel increase in species (*Pinus*, mountain trees and herbs) indicating cooler climatic conditions (Amorosi *et al.*, 2008). Two mud horizons, which record the maximum expansion of warmth-loving forests, were assigned to MIS 7 and MIS 5e (Fig. 6) based on stratigraphic correlations with coeval

coastal sediments (Campo *et al.*, 2020). Compositional data from cores MED, MIR and CNC show that channel-belt sand bodies numbered as ‘2’ to ‘4’ in Fig. 6, *ca* 30 km wide, were deposited by the Po River flowing in an axial position. The oldest sand body of unit UPS (number ‘1’ in Fig. 6) is preserved only within a syncline. The youngest sand body results from the amalgamation of channel complexes 4a and 4b (Fig. 6) mainly accumulated during the last glacial episode. Towards the north, Po River sands are laterally juxtaposed with sand bodies deposited by Alpine rivers (see cores EM19 and MN1; Fig. 6). Towards the south, 35 to 40 km from the Apennine foothills, Po sands pass to floodplain muds delivered by the Apennine rivers. In this mud-prone succession, the physical tracking of palaeosols was possible only within the upper 50 m, where high-quality core data are available (see *Late Pleistocene–Holocene*

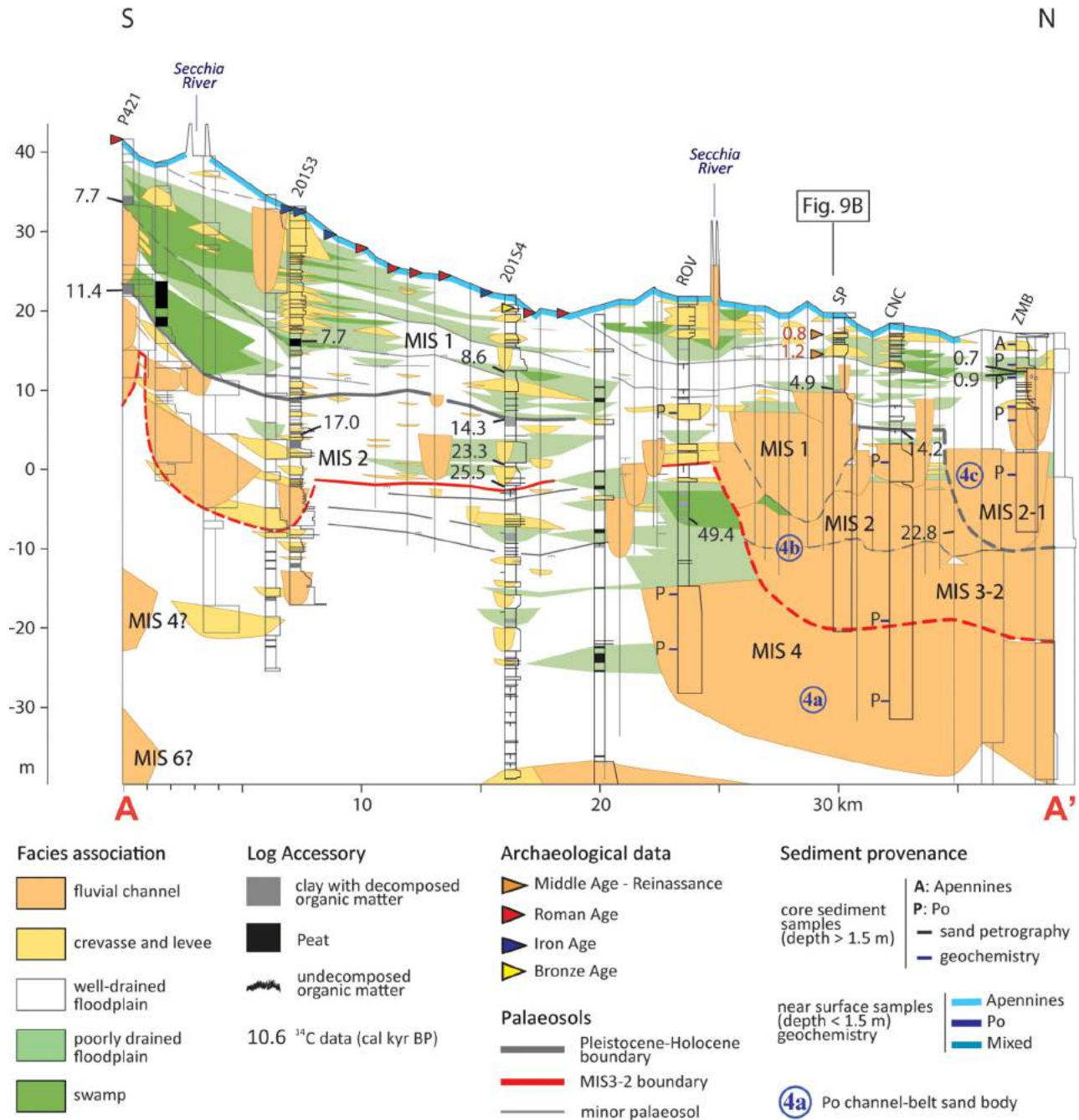


Fig. 7. Late Pleistocene stratigraphic architecture of the central Po Plain along a north–south-oriented profile (modified after Amorosi *et al.*, 2016). Location in Fig. 2. Provenance interpretation of near-surface sediments (depth <1.5 m) is from Amorosi *et al.* (2014).

stratigraphy section). Fluvial–channel lenses deposited by Apennine rivers (see provenance data from cores Modena, TAV181, CV1 and CV3, Fig. 6) are generally thinner and narrower than the Po-sourced sediment bodies. A thin, organic-matter-rich horizon marks the base of

MIS 5e deposits (Fig. 6). At depth >50 m, basal surfaces of subsynthem can be tracked only tentatively due to poor quality of well-log descriptions (see dashed lines in Fig. 6). A recurrent alternation of coarse and fine-grained sediments is also observed close to the

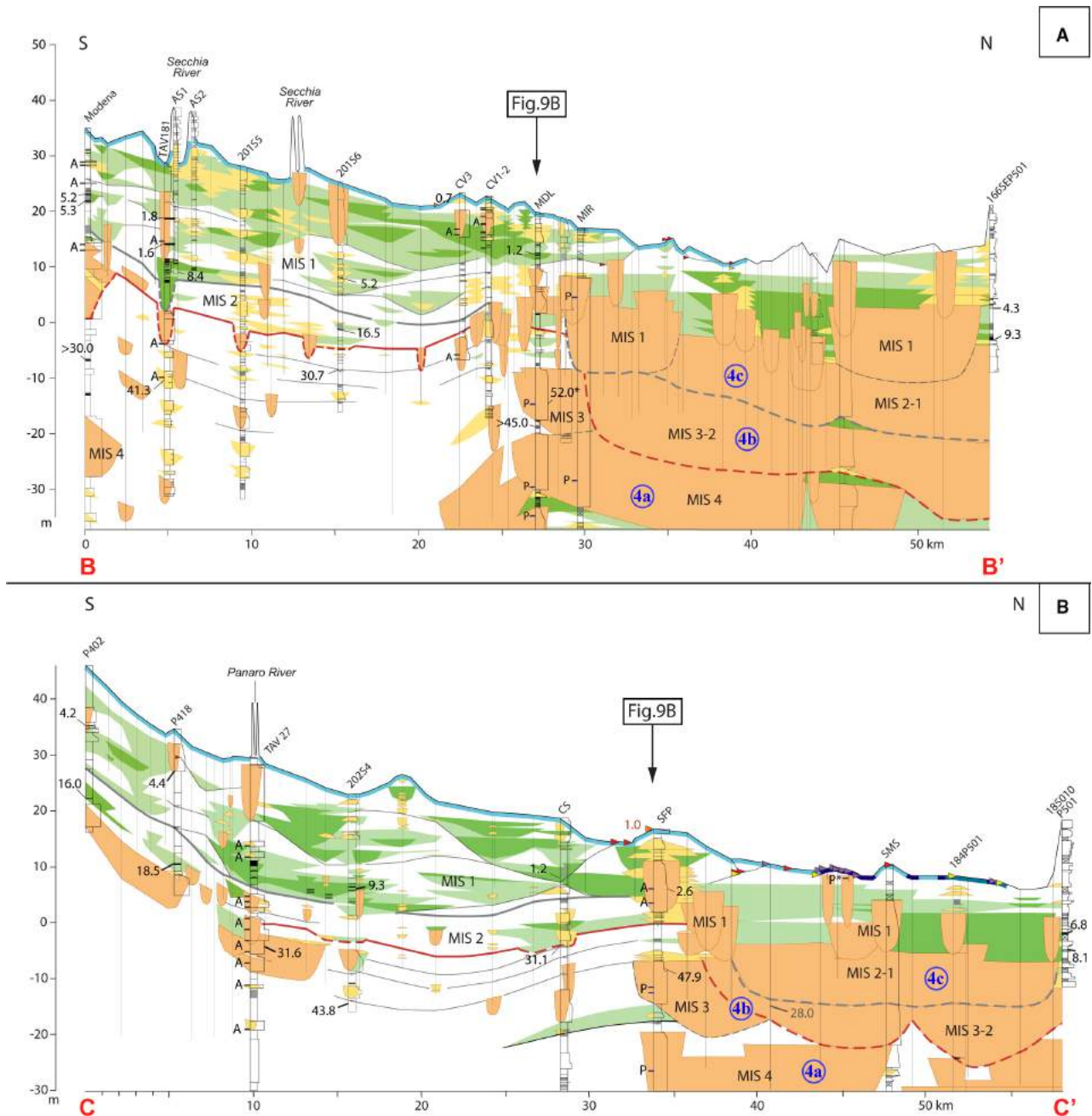


Fig. 8. Late Pleistocene stratigraphic architecture of the central Po Plain along two north–south-oriented profiles. Location in Fig. 2. For legend see Fig. 7. The date marked with an asterisk is not calibrated. The date in grey is projected from a nearby core.

Apennine margin, where vertically stacked gravel bodies are the dominant feature.

Alluvial deposits of the Lower Po Synthem (LPS in Fig. 6) are folded and pinch out towards the culmination of the Mirandola anticline, where they are less than 10 m thick. Compositional data from cores MED and MIR show a

strong affinity with modern Alpine rivers, such as Oglio and Mincio (Amorosi & Sammartino, 2018). The coeval Po fluvial-channel sediments likely correspond to two sand bodies encountered in well Carpi1, *ca* 25 km north of the Apennine foothills, at *ca* 360 m and 250 m depth ('A' and 'B' in Fig. 6, respectively), which

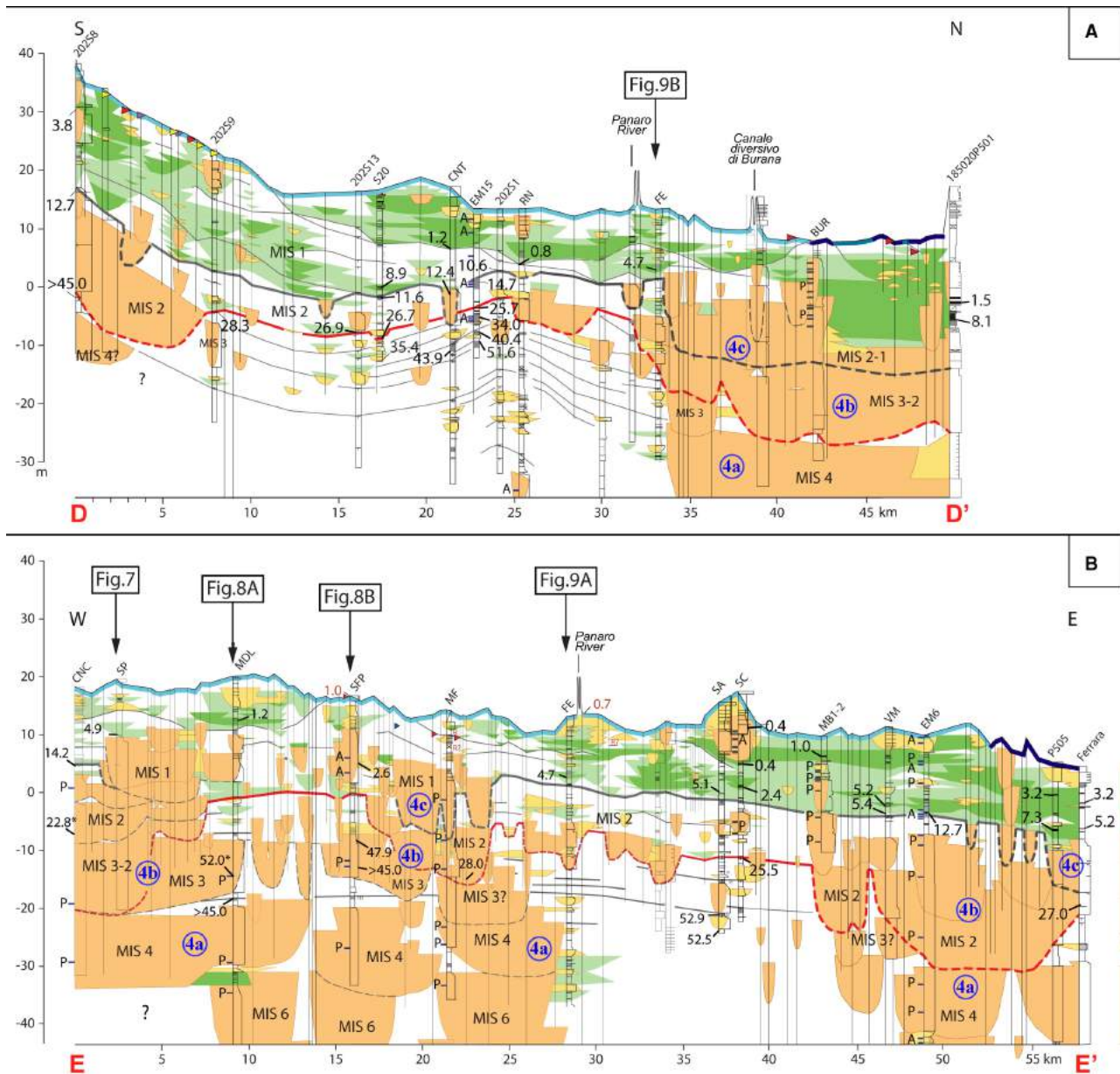


Fig. 9. Late Pleistocene stratigraphic architecture of the central Po Plain along a north–south-oriented profile (A) and a west–east-oriented transect (B). Location in Fig. 2. For legend see Fig. 7. Petrographic data from core BUR are from Amoroso *et al.* (2020).

have thicknesses of *ca* 30 m, consistent with UPS Po channel-belt sand bodies.

Late Pleistocene–Holocene stratigraphy

The Late Pleistocene–Holocene stratigraphy is explored here to unravel the mutual relations between the Po River and its southern tributaries across the last glacial cycle and the Present Interglacial.

In the northern part of the study area, a 40 m thick channel-belt sand body was encountered at depths >10 m (Figs 7, 8 and 9) and tracked continuously along strike for at least 30 km. Its southern boundary is located *ca* 20 km south of the modern Po River. Petrographic and geochemical data from 89 samples indicate sediment supply from the Po River (stratigraphic position of samples in Figs 7, 8 and 9). The local occurrence

of thin mud lenses permits its subdivision in three smaller-scale aggradationally stacked sand bodies ('4a', '4b' and '4c' in Figs 7, 8 and 9). Based on sparse radiocarbon data and on the stratigraphic relations with overlying and underlying organic-matter-rich horizons, sand body 4b accumulated during MIS 3 and MIS 2 (between *ca* 52 and 14 kyr BP), whereas 4c was dated to the MIS 2 – MIS 1 transition (*ca* 14–9 kyr BP). Sand body 4a is tentatively assigned to MIS 4 based on the correlation scheme of Fig. 6. Thicker and more laterally persistent mud strata separate 4a from 4b (Fig. 9B). Older sand bodies attributed to MIS 6 are locally encountered at the bottom section in Fig. 9B.

Holocene (MIS 1) sand bodies are vertically amalgamated onto older sands and show lateral transition to muddy facies associations (Figs 7, 8 and 9). These sand bodies were deposited by the Po River (cores ZMB, SP, BUR and MB1-2) and by Apennine tributaries (SFP and SC1-2). Holocene mud-prone deposits in core EM6 (Fig. 9B) show alternating contributions from Po and Apennine sediments sources.

South of the Po channel belt, muds are dominant and fluvial-channel bodies are lens-shaped (Figs 7, 8, and 9). Fifty-three compositional data denote an Apennine sediment provenance. Laterally extensive gravel and sand sheets were encountered only at the southern edge of the study area. The Late Pleistocene interval, almost entirely composed of *WDF* muds, is marked by laterally extensive (>20 km) Inceptisols, locally replaced by coeval fluvial-channel deposits or eroded by younger channels. Two palaeosols, dated to 29–25 and 14.7–10.6 kyr BP (bold red and grey lines respectively in Figs 7, 8, and 9), mark the base of MIS 2 and MIS 1 deposits (Figs 7, 8 and 9). The 'red' palaeosol caps a series of closely spaced palaeosols that are radiocarbon dated to MIS 3. The 'grey' palaeosol marks the Pleistocene–Holocene boundary. The elevation of the Late Pleistocene palaeosols is highest close to the Apennine foothills and above the culmination of the Mirandola anticline. The MIS 3 palaeosol-bounded units are thin (<2 m) and nearly tabular. The unit bounded by the 'red' and 'grey' palaeosols is 4 to 12 m thick, with minimum values above the Mirandola Anticline (Figs 7, 8 and 9).

Holocene palaeosols are typically discontinuous, more immature (Entisols), and bound lens-shaped mud-dominated units with convex-up upper boundaries and maximum thickness of 12

to 15 m. *PDF*, *SW* and *CL* facies are abundant. *FC* facies are isolated and of small lateral extent.

DISCUSSION

Middle Pleistocene evolution of Po and Apennine river systems

Vertically stacked channel-belt sand bodies are the dominant features of Middle and Late Pleistocene stratigraphy in the central Po Plain. Radiocarbon dates from the uppermost sand body ('4b' in Fig. 6) indicate its accumulation during the last glacial stage. Deposition of older channel-belt sand bodies during glacial stages is demonstrated by the increase in pollen from taxa typical of cold climates at the upward transition from mud-prone strata to laterally extensive sand bodies (Vittori & Ventura, 1995; Amorosi *et al.*, 2008). The presence of four channel belt sand bodies ('1' to '4', Fig. 6) above a surface dated to *ca* 450 kyr BP (Martelli *et al.*, 2017) suggests their deposition during the last four glacial stages (i.e. MIS 10, 8, 6 and 4-2). This age attribution is supported by the correlation with fluvial-channel bodies exposed in the Enza section, just 30 km west of the study area (location in Fig. 10), which accumulated at glacial culminations (Gunderson *et al.*, 2014). The age of channel belts A and B is constrained between the ages of the basal and upper surface of the Lower Po Synthem (870 kyr and 450 kyr, Muttoni *et al.*, 2003; Gunderson *et al.*, 2014; Martelli *et al.*, 2017) regionally mapped on a seismic basis. Sand body 'B', overlain by the 450 kyr surface, was tentatively assigned to MIS 12, based on stratigraphic correlation with coeval channel bodies exposed in the Enza Section (Gunderson *et al.* 2014). A palaeo-Po River course flowing closer to the Apennine chains has also been postulated by Garzanti *et al.* (2011), who documented a southward progradation of Alpine fans during MIS 12.

The location of boundaries between Po and Apennine deposits, identifiable within glacial stratigraphic intervals as a mud–sand contact, fluctuated in a north–south direction during the last 870 kyr. Lateral shifts <10 km are recorded from MIS 8 to the Present (see sand bodies '2', '3', '4a' and '4b', Fig. 6), whereas a northward shift of more than 20 km is recorded across the 450 kyr unconformity (from B to 1, Fig. 6). Alpine sediments from the LPS in cores MED

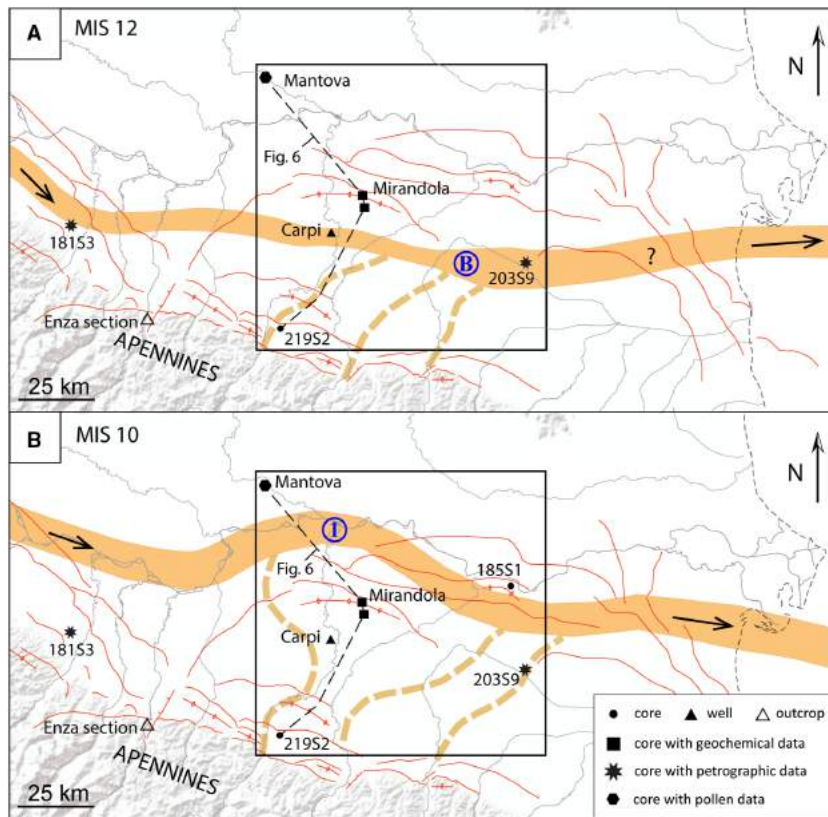


Fig. 10. Palaeogeographic sketch maps showing the northward shift of the Po channel belt (in orange) around 450 kyr BP. Inferred Apennine palaeochannels are represented through orange dashed lines. Petrographic data from cores 181S3 and 203S9 are from Ceriani & Di Giulio (2008) and Albertini *et al.* (2009), respectively. Chronological data from the Enza section are from Gunderson *et al.* (2014). The arrow represents the Po palaeoflow direction. Location of cross-section of Fig. 6 is also indicated (black dashed line). 'B' and '1' are channel-belt names as in Fig. 6.

and MIR (Amorosi & Sammartino, 2018) indicate that the Po River flowed south of the Mirandola anticline (*ca* 30 km south of the modern Po River) before 450 kyr BP (Fig. 10A). This reconstruction is corroborated by compositional data reported in previous studies, which documented the presence of Po sands close to the Apennine foothills (cores 181S3 and 203S9 in Fig. 10; Ceriani & Giulio, 2008; Albertini *et al.*, 2009). Sand body '1', tentatively attributed to MIS 10, is confined north of the Mirandola thrusts (Figs 6 and 10B). Interestingly, Apennine sediments were not encountered in cores MED and MIR. Thus, this area was bypassed by the Apennine rivers during MIS 10 (Fig. 10). Alternatively, the Apennine sediments were not preserved at the anticlinal culmination. The preservation of oldest UPS deposits only within syncline structures and onlapping geometries onto the UPS lower boundary (Fig. 6) testify to a possible accelerated growth of the Mirandola Anticline around 450 kyr BP, at the LPS–UPS transition. In contrast, trunk-river sedimentation spread above the anticline culmination since at least MIS 8 (see sand bodies 2 to 4b, Figs 6 and

11), suggesting a possible decelerated anticline growth.

Late Pleistocene and Holocene evolution of the Po and Apennine river systems

The great thickness of the Po alluvial succession (up to 420 m in last 870 kyr, Fig. 6), the aggradational stacking of channel-belt sand bodies, and the relatively poor development of palaeosols reflect high subsidence rates (Posamentier & Vail, 1988; Wright & Marriott, 1993; Blum *et al.*, 2013) that exceed 2 mm/yr in syncline and coastal plain areas (Carminati & Martinelli, 2002; Bruno *et al.*, 2017b). In these depocentres, a thick (up to 70 m) sediment succession accumulated during the last glacial episode (Fig. 6; see also Campo *et al.*, 2020). Within this overall high-accommodation trend, vertical changes in: (i) fluvial-channel stacking patterns; (ii) lateral extent, maturity and continuity of palaeosols; and (iii) relative proportion of poorly drained floodplain and swamp facies, reflect variations in accommodation linked to the climatic–eustatic history of the area. The Late Pleistocene

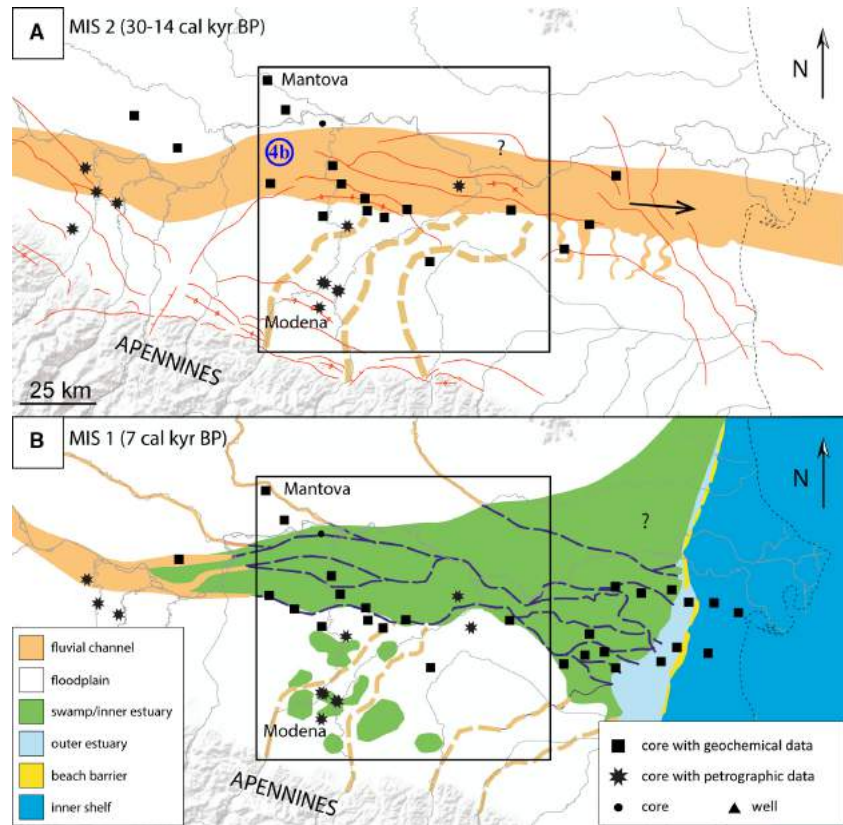


Fig. 11. (A) Palaeogeography of the Po Plain during MIS 2, between 30 and 14 cal kyr BP. Stratigraphic and compositional data beyond the study area are from Bruno *et al.* (2017a, 2018). The arrow represents the Po palaeoflow direction. (B) Palaeogeography of the Po Plain during MIS 1, at maximum marine ingression (modified after Amorosi *et al.*, 2017b). Dashed lines represent the inferred location of Po distributary channels (in blue) and of Apennine tributaries (in orange). The dotted line represents the present-day Adriatic coastline.

succession records a progressive widening of the Po channel belt towards the glacial culmination, from MIS 4 (sand body '4a', Figs 6 and 12) to MIS 3–MIS 2 ('4b', Figs 6 and 12). Sand body 4b accumulated in a high-sediment supply setting due to its connection with the Alpine fluvio-glacial system (Fontana *et al.*, 2014) and can be correlated from west to east for more than 120 km (Campo *et al.*, 2016; Amorosi *et al.*, 2017a; Bruno *et al.*, 2017a). Laterally continuous channel-belt sand bodies from ancient (Labourdette & Jones, 2007) and late Quaternary successions ('amalgamated valley fills' of Blum *et al.*, 2013) have been commonly reported in continental sequence stratigraphic models, as part of the 'low accommodation systems tract' (Wright & Marriott, 1993; Currie, 1997; Caturanu *et al.*, 2009). In the Late Pleistocene succession of the Po Plain, low accommodation is also demonstrated by low sedimentation rates (Bruno *et al.* 2017b) and the lateral association of sand body 4b with a set of closely spaced Inceptisols with great lateral continuity, which developed in a well-drained environment. Similar series of vertically stacked, aggradational palaeosols bracketing the sequence boundary

(McCarthy & Plint, 2013) have been described as 'soil zones' (Morton & Suter, 1996), 'pedocomplexes' (Hanneman & Wideman, 2006, 2010) or 'fluvial aggradational cycles' (Atchley *et al.*, 2013). The widening of the Po channel-belt resulted in the cannibalization of mud deposits, which were transferred 400 km downstream of the study area to the lowstand prograding complex (Pellegrini *et al.*, 2018), and in the reduction of the potential area for Apennine-rivers sedimentation. Preserved Apennine sediments are thin palaeosol-bounded overbank strata, whose deposition was controlled by millennial-scale climate oscillations (Bruno *et al.*, 2020a). From the analysis of 80 radiocarbon dated soil profiles, Bruno *et al.* (2020a) documented that palaeosol burial occurred during cold periods, when a more open herbaceous vegetation favoured erosion in the Apennine drainage basins and sediment transfer to the alluvial plains.

The post-glacial succession, between 14 and 10 kyr BP, records the progressive expansion of the Apennine sedimentation area due to the narrowing of the Po channel ('4c' in Fig. 12). That narrowing was the result of sediment trapping

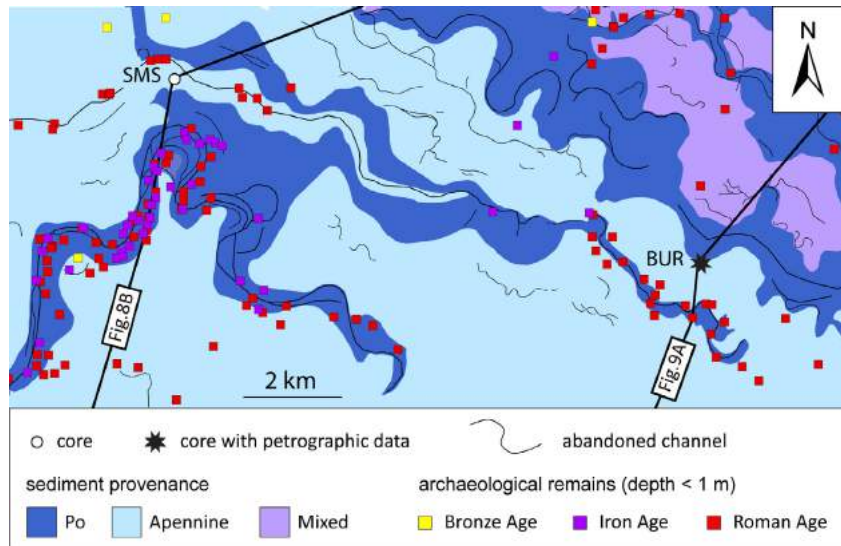


Fig. 13. Sediment provenance of Late Holocene exposed sediments showing lateral juxtaposition of the Po and Apennine deposits (modified after Amorosi *et al.*, 2014). Location in Fig. 2.

Controlling factors of trunk-tributary river shifts and implications for fine versus coarse-grained sediment storage

In large alluvial systems, trunk rivers are commonly regarded as the main agents of sediment deposition, whereas the contribution of tributaries is considered highly subordinate (Aslan & Autin, 1999; Busschers *et al.*, 2007). Recent works highlight the role of tributary rivers in the evolution of alluvial and coastal-plain landscapes (Aalto *et al.*, 2003; Fielding *et al.*, 2012; Simms & Rodriguez, 2015; Tentori *et al.*, 2021) and in the storage of fine-grained material (Kvale & Archer, 2007; Vis *et al.*, 2008). In the Po valley, which in the study area extends for 90 km along strike, transverse tributaries have considerable space for the deposition of sediment supplied by two active orogens (i.e. Southern Alps and Northern Apennines) parallel to the trunk river. A similar configuration characterizes the Ganges system, where tributaries draining the Himalayan belt (Singh *et al.*, 2008) and the Indian Craton (Sinha *et al.*, 2009) supply considerable amounts of sediment to the mainstream. The alluvial record of the Po Basin hosts evidence of episodic lateral shift of the Po River over the last 870 kyr, with consequent enlargement or shrinking of the South-Alpine and Apennine river domains. Of particular interest is the boundary between the Po and the Apennine sedimentary areas because it is marked by a sharp change in grain-size (Figs 6 to 9) and sediment composition (Figs 4 and 5). This boundary was displaced in a south–north

direction by three main processes that acted at different timescales and responded to distinctly different controlling factors.

1 A northward shift of the Po channel belt by more than 20 km at the MIS 12–MIS 11 transition (Figs 6 and 10), implied a substantial enlargement of the Apennine domain, with the accumulation of considerable amounts of fine-grained material from then onward. A structural control is proposed for this reorganization of the fluvial network, recorded across a regional unconformity characterized by onlap contacts in the study area (Fig. 6) and in other parts of the basin (Martelli *et al.*, 2017). The LPS–UPS boundary, dated to the MIS 12–MIS 11 transition, also corresponds to a marine transgression at termination V (Lisiecki & Raymo, 2005) which may also have contributed to a substantial reorganization of the river network. Further chronological, palaeogeographical and structural data are required to discriminate the relative role of eustasy and tectonics.

2 Changes in the width of the Po channel belt driven by glacial–interglacial climate oscillations resulted in a periodic variation of the area available for Apennine rivers sedimentation. High sediment supply from the Alpine fluvio-glacial and Apennine river systems and low accommodation during falling stage–lowstand periods resulted in widening of the channel-belt and its displacement towards the Apennine domain. These climatically induced variations resulted in lateral shifts of the boundary between the Po and the Apennine domains of less than 10 km (Fig. 10).

3 During interglacial periods, nodal avulsions of the trunk river resulted in sharp widening and narrowing of the area available for Apennine river sedimentation. These variations at the 10^2 – 10^3 yr timescale are highlighted within single cores by the alternation of deposits with contrasting composition (core EM6, Fig. 9B) and by the presence of Apennine ribbons within the Po sedimentary domains (Fig. 13). This study argues for a dominant autogenic control on Po River avulsions during the Holocene (Amorosi *et al.*, 2017b), although short-lived climate oscillations may have enhanced river instability in some periods (Cremonini *et al.*, 2013).

CONCLUSIONS

Interaction of tributaries with a trunk river can influence grain-size distribution and composition of sediment stored in alluvial plains. In the Po Plain, the main river deposited aggradationally stacked sand bodies, 20 to 30 km wide and up to 40 m thick, separated by overbank mud strata. Po sands show high contents in quartz–feldspar and metamorphic rock fragments, combined with high chromium levels. To the south, Apennine deposits are coarse-grained only close to their valley outlets, where they form laterally continuous gravel and sand bodies. Downstream, muds are dominant, and sands are confined in narrow ribbons. Sands delivered by Apennine rivers are readily distinguishable from the Po sands due to their lower quartz–feldspar content, abundant sedimentary lithics and lower chromium levels.

From 870 to 450 kyr BP, when the Po River flowed close to the Apennine chain, Apennine river deposition was restricted to a relatively narrow area. Soon after 450 kyr BP, the Po channel belt shifted northward by more than 20 km, probably in response to a prominent tectonic event. Since then, Apennine rivers have deposited large volumes of fine-grained material over a considerably larger area than before.

This area periodically narrowed and enlarged in response to glacial–interglacial oscillations. In particular, Po channel-belt widening during glacial periods reduced the area for Apennine rivers sedimentation. A 25 to 30 km wide channel-belt sand body was deposited by the Po River between *ca* 52 and 14 kyr BP. Coeval Apennine muds to the south are punctuated by vertically stacked Inceptisols that attest to short-lived

phases of no sedimentation driven by millennial-scale climate oscillations.

The post-glacial succession records the progressive narrowing of the Po channel belt and the transition to an avulsive–distributive Po River pattern in the study area. Narrow (<3 km) channel belts formed along the Po River branches and abundant swamp and poorly drained-floodplain muds were preserved in interfluvial areas. The temporary deactivation of the southernmost Po river branches resulted in the sharp widening of the area available for Apennine river sedimentation and permitted the intrusion of Apennine sediments in the former domain of the Po River. Alternating sedimentation from the Po and the Apennine rivers is recorded at the boundary between the two domains, where sediments with contrasting petrographic and geochemical signatures are vertically superposed or laterally juxtaposed.

Combined stratigraphic and sediment provenance analyses are particularly effective in the investigation of Quaternary alluvial successions, where the reconstructions of the patterns of sediment dispersal typically rely upon a robust chronology, a detailed knowledge of the drainage system and reliable sediment-provenance markers.

ACKNOWLEDGEMENTS

We gratefully acknowledge L. Martelli for access to the cores analysed in this work and R. Caputo for access to the San Carlo trench. This paper was improved by the constructive suggestions of reviewers Stacey Atchley, Hans Middelkoop, and Salvatore Milli and of Associate Editor Christopher R. Fielding. A special thanks to Kevin Bohacs for a careful revision of the manuscript.

DATA AVAILABILITY STATEMENT

This research relied upon a stratigraphic dataset, available online at <https://ambiente.regione.emilia-romagna.it/it/geologia/cartografia/webgis-banchedati/webgis-e-banche-dati> and <https://www.videpi.com/videpi/videpi.asp>, and on radiocarbon dates available in the Data S1.

The *Pedogeochemical Map of Regione Emilia-Romagna* is available on line (<https://ambiente.regione.emilia-romagna.it/it/geologia/cartografia/webgis-banchedati/webgis-suoli>).

REFERENCES

- Aalto, R., Maurice-Bourgoin, L., Dunne, T., Montgomery, D.R., Nittrouer, C.A. and Guyot, J.L. (2003) Episodic sediment accumulation on Amazonian floodplains influenced by El Niño/Southern Oscillation. *Nature*, **425**, 493–497.
- Abels, H.A., Kraus, M.J. and Gingerich, P.D. (2013) Precession-scale cyclicity in the fluvial lower Eocene Willwood Formation of the Bighorn Basin, Wyoming (USA). *Sedimentology*, **60**, 1467–1483.
- Albertini, C., Ceriani, A. and Di Giulio, A. (2009). Petrografia delle Sabbie di Sottosuolo. In: *Note illustrative della carta geologica d'Italia alla scala 1:50.000, foglio 203 Poggio Renatico* (Eds Cibin, U. and Segadelli, S.), pp. 104. SystemCart, Roma.
- Alexander, C.S. and Prior, J.C. (1971) Holocene sedimentation rates in overbank deposits in the Black Bottom of the lower Ohio River, southern Illinois. *Am. Jour. Sci.*, **270**, 361–372.
- Allen, J.R.L. (1963) The classification of cross-stratified units with notes on their origin. *Sedimentology*, **2**, 93–114.
- Amadori, C., Toscani, G., Di Giulio, A., Maesano, F.E., D'Ambrogi, C., Ghielmi, M. and Fantoni, R. (2019) From cylindrical to non-cylindrical foreland basin: Pliocene-Pleistocene evolution of the Po Plain-Northern Adriatic basin (Italy). *Basin Res.*, **31**(5), 991–1015.
- Amorosi, A., Bruno, L., Facciorusso, J., Piccin, A. and Sammartino, I. (2016) Stratigraphic control on earthquake-induced liquefaction: a case study from the Central Po Plain (Italy). *Sed. Geol.*, **345**, 42–53.
- Amorosi, A., Bruno, L., Cleveland, D.M., Morelli, A. and Hong, W. (2017a) Paleosols and associated channel-belt sand bodies from a continuously subsiding late Quaternary system (Po Basin, Italy): new insights into continental sequence stratigraphy. *Geol. Soc. Am. Bull.*, **129**, 449–463.
- Amorosi, A., Bruno, L., Campo, B., Morelli, A., Rossi, V., Scarponi, D., Hong, W., Bohacs, K.M. and Drexler, T.M. (2017b) Global sea-level control on local parasequence architecture from the Holocene record of the Po Plain, Italy. *Mar. Pet. Geol.*, **87**, 99–111.
- Amorosi, A., Colalongo, M.L., Fiorini, F., Fusco, F., Pasini, G., Vaiani, S.C. and Sarti, G. (2004) Palaeogeographic and palaeoclimatic evolution of the Po Plain from 150-ky core records. *Glob. Planet. Change*, **40**, 55–78.
- Amorosi, A., Guermandi, M., Marchi, N. and Sammartino, I. (2014) Fingerprinting sedimentary and soil units by their natural metal contents: a new approach to assess metal contamination. *Sci. Total Environ.*, **500–501**, 361–372.
- Amorosi, A., Pavesi, M., Ricci Lucchi, M., Sarti, G. and Piccin, A. (2008) Climatic signature of cyclic fluvial architecture from the Quaternary of the central Po Plain, Italy. *Sed. Geol.*, **209**, 58–68.
- Amorosi, A. and Sammartino, I. (2007) Influence of sediment provenance on background values of potentially toxic metals from near-surface sediments of Po coastal plain (Italy). *Int. J. Earth Sci.*, **96**, 389–396.
- Amorosi, A. and Sammartino, I. (2018) Shifts in sediment provenance across a hierarchy of bounding surfaces: A sequence-stratigraphic perspective from bulk-sediment geochemistry. *Sed. Geol.*, **375**, 145–156.
- Amoroso, S., Rollins, K.M., Andersen, P., Gottardi, G., Tonni, L., García Martínez, M.F., Wissmann, K., Minarelli, L., Comina, C., Fontana, D., De Martini, P.M., Monaco, P., Pesci, A., Sapia, V., Vassallo, M., Anzidei, M., Carpena, A., Cinti, F., Civico, R., Coco, I., Conforti, D., Doumaz, F., Giannatasio, F., Di Giulio, G., Foti, S., Loddo, F., Lugli, S., Manuel, M.R., Marchetti, D., Mariotti, M., Materni, V., Metcalfe, B., Milana, G., Pantosti, D., Pesce, A., Salocchi, A.C., Smedile, A., Stefani, M., Tarabusi, D. and Teza, G. (2020) Blast-induced liquefaction in silty sands for full-scale testing of ground improvement methods: Insights from a multidisciplinary study. *Eng. Geol.*, **265**, 105437.
- Aslan, A. and Autin, W.J. (1999) Evolution of the Holocene Mississippi River floodplain, Ferriday, Louisiana: insights of the origin of fine-grained floodplains. *J. Sedim. Res.*, **69**, 800–815.
- Atchley, S.C., Nordt, L.C., Dworkin, S.I., Cleveland, D.M., Mintz, J.S. and Hunter Harlow, R. (2013). Alluvial stacking pattern analysis and sequence stratigraphy: Concepts and case studies. In: *New Frontiers in Paleopedology and Terrestrial Paleoclimatology: Paleosols and Soil Surface Analog Systems* (Eds Driese, S.C., Nordt, L.C. and McCarthy, P.J.), *Society for Sedimentary Geology Special Publication*, **104**, 109–129.
- Biancardi, D. (2013). *Carta archeologica del territorio di Bondeno (Ferrara) dalla Preistoria all'Età moderna*. Unpublished thesis, 279 pp. (in Italian).
- Bishop, P. (1995) Drainage rearrangement by river capture, beheading and diversion. *Progress in Physical Geography: Earth and Environment*, **19**, 449–473.
- Blum, M.D. and Aslan, A. (2006) Signatures of climate vs. sea-level change within incised valley successions: quaternary examples from the Texas Coastal Plain and Shelf. *Sediment. Geol.*, **190**, 177–211.
- Blum, M.D., Martin, J., Milliken, K. and Garvin, M. (2013) Paleovalley systems: Insights from Quaternary analogs and experiments. *Earth Sci. Rev.*, **116**, 128–169.
- Blum, M.D. and Törnqvist, T.E. (2000) Fluvial response to climate and sea-level change: a review and look forward. *Sedimentology*, **47**(Suppl.), 1–48.
- Boccaletti, M., Corti, G. and Martelli, L. (2011) Recent and active tectonics of the external zone of the Northern Apennines (Italy). *Int. J. Earth Sci.*, **100**, 1331–1348.
- Bonini, L., Toscani, G. and Seno, S. (2014) Three-dimensional segmentation and different rupture behavior during the 2012 Emilia seismic sequence (Northern Italy). *Tectonophysics*, **630**, 33–42.
- Briant, R.B., Bateman, M.D., Coope, G.R. and Gibbard, P.L. (2005) Climatic control on Quaternary fluvial sedimentology of a Fenland Basin river, England. *Sedimentology*, **52**, 1397–1423.
- Bridge, J.S. (1993). The interaction between channel geometry, water flow, sediment transport and deposition in braided rivers. In: *Braided Rivers* (Eds Best, J.L. and Bristow, C.S.), *Geol. Soc. Lond. Spec. Publ.*, **75**, 13–71.
- Bronk Ramsey, C. and Lee, S. (2013) Recent and planned developments of the program OxCal. *Radiocarbon*, **55**, 720–730.
- Bruno, L., Amorosi, A., Severi, P. and Costagli, B. (2017a) Late Quaternary aggradation rates and stratigraphic architecture of the southern Po Plain, Italy. *Basin Res.*, **29**, 234–248.
- Bruno, L., Bohacs, K.M., Campo, B., Drexler, T.M., Rossi, V., Sammartino, I., Scarponi, D., Hong, W. and Amorosi, A. (2017b) Early Holocene transgressive paleogeography in the Po coastal plain (northern Italy). *Sedimentology*, **64**(7), 1792–1816.

- Bruno, L., Campo, B., Costagli, B., Stouthamer, E., Teatini, P., Zoccarato, C. and Amorosi, A. (2020) Factors controlling natural subsidence in the Po Plain. *Proc. Int. Assoc. Hydrol. Sci.*, **382**, 285–290.
- Bruno, L., Marchi, A., Bertolini, I., Gottardi, G. and Amorosi, A. (2020a) Climate control on stacked paleosols in the Pleistocene of the Po Basin (northern Italy). *J. Quat. Sci.*, **35**(4), 559–571.
- Bruno, L., Piccin, A., Sammartino, I. and Amorosi, A. (2018) Decoupled geomorphic and sedimentary response of Po River and its Alpine tributaries during the last glacial/post-glacial episode. *Geomorphology*, **317**, 184–198.
- Buol, S.W., Southard, R.J., Graham, R.C. and McDaniel, P.A. (2011) *Soil Genesis and Classification*, 6th edn. Wiley-Blackwell, Chichester, 543 p. <https://doi.org/10.1002/9780470960622>.
- Busschers, F.S., Kasse, C., van Balen, R.T., Vandenberghe, J., Cohen, K.M., Weerts, H.J.T., Wallinga, J., Johns, C., Cleveringa, P. and Bunnik, F.P.M. (2007) Late Pleistocene evolution of the Rhine-Meuse system in the southern North Sea basin: imprints of climate change, sea-level oscillation, and glacio-isostasy. *Quat. Sci. Rev.*, **26**, 3216–3248.
- Busschers, F.S., Weerts, H.J.T., Wallinga, J., Cleveringa, P., Kasse, C., de Wolf, H. and Cohen, K.M. (2005) Sedimentary architecture and optical dating of middle and late Pleistocene Rhine-Meuse deposits—Fluvial response to climate change, sea-level fluctuation and glaciation. *Neth. J. Geosci.*, **84**(1), 25–41.
- Caldarelli, A. and Malnati, L. (2003). *Atlante dei beni archeologici della Provincia di Modena, Volume 1*. All'Insegna del Giglio, Pianura, 227 pp.
- Campanella, R.G., Gillespie, D. and Robertson, P.K. (1982). Pore pressures during cone penetration testing. *Proc. 2nd Eur. Symp. Penetration Testing, ESOPT, IICloseCheck*, 507–512.
- Campo, B., Amorosi, A. and Bruno, L. (2016) Contrasting alluvial architecture of late Pleistocene and Holocene deposits along a 120-km transect from the central Po Plain (northern Italy). *Sediment. Geol.*, **341**, 265–275.
- Campo, B., Bruno, L. and Amorosi, A. (2020) Basin-scale stratigraphic correlation of late Pleistocene-Holocene (MIS 5e-MIS 1) strata across the rapidly subsiding Po Basin (northern Italy). *Quatern Sci. Rev.*, **237**, 106300.
- Caputo, R., Iordanidou, K., Minarelli, L., Papanthassiou, G., Poli, M.E., Rapti-Caputo, D., Sboras, S., Stefani, M. and Zanferrari, A. (2012) Geological evidence of pre-2012 seismic events, Emilia-Romagna, Italy. *Ann. Geophys.*, **55**, 743–749.
- Carminati, E. and Doglioni, C. (2012) Alps vs. Apennines: the paradigm of a tectonically asymmetric Earth. *Earth Sci. Rev.*, **112**, 67–96.
- Carminati, E. and Martinelli, G. (2002) Subsidence rates in the Po Plain, northern Italy: the relative impact of natural and anthropogenic causation. *Eng. Geol.*, **66**, 241–255.
- Catuneanu, O., Abreu, V., Bhattacharya, J.P., Blum, M.D., Dalrymple, R.W., Eriksson, P.G., Fielding, C.R., Fisher, W.I., Galloway, W.E., Gibling, M.R., Giles, K.A., Holbrook, J.M., Jordan, R., Kendall, C.G.S.C., Macurda, B., Martinsen, O.J., Miall, A.D., Neal, J.E., Nummedal, D., Pomar, L., Posamentier, H.W., Pratt, B.R., Sarg, J.F., Shanley, K.W., Steel, R.J., Strasser, A., Tucker, M.E. and Winker, C. (2009) Towards the standardization of sequence stratigraphy. *Earth-Sci. Rev.*, **92**, 1–33.
- Ceriani, A. and Di Giulio, A. (2008). Petrografia delle Sabbie di Sottosuolo. In: *Note illustrative della carta geologica d'Italia alla scala 1:50.000, foglio 203 Poggio Renatico* (Ed. Calabrese, L.), pp. 76. S.EL.CA. s.r.l., Firenze.
- Cleveland, D.M., Atchley, S.C. and Nordt, L.C. (2007) Continental sequence stratigraphy of the Upper Triassic (Norian-Rhaetian) Chinle strata, northern New Mexico, U.S.A.: Allocyclic and autocyclic origins of paleosol-bearing alluvial successions. *J. Sediment. Res.*, **77**(11), 909–924.
- Collinson, J.D. (1978) Alluvial sediments. In: *Sedimentary Environments and Facies* (Ed. Reading, H.G.), 2nd edn, pp. 20–67. Blackwell, Oxford.
- Cremonini, S., Labate, D. and Curina, R. (2013) The late-antiquity environmental crisis in Emilia region (Po river plain, Northern Italy): Geoarchaeological evidence and paleoclimatic considerations. *Quatern. Int.*, **316**, 162–178.
- Currie, B.S. (1997) Sequence stratigraphy of nonmarine Jurassic-Cretaceous rocks, central Cordilleran foreland basin system. *Geol. Soc. Am. Bull.*, **109**, 120621222.
- Dansgaard, W., Johnsen, S., Clausen, H.B., Dahl-Jensen, D., Gundestup, D.S., Hammer, C.U., Hvidberg, C.S., Steffensen, J., Sveinbjörnsdóttir, A.E., Jouzel, J. and Bond, G. (1993) Evidence for general instability of past climate from a 250 kyr ice-core record. *Nature*, **364**, 218–220.
- Devoti, R., Esposito, A., Pietrantonio, G., Pisani, A.R. and Riguzzi, F. (2011) Evidence of large scale deformation patterns from GPS data in the Italian subduction boundary. *Earth Planet. Sci. Lett.*, **311**, 230–241.
- Diessel, C.F.K. (Ed.). (1992) Coal facies and depositional environment. In: *Coal-Bearing Depositional Systems* pp. 161–264. Springer, Berlin.
- DISS Working Group. (2018). Database of individual seismogenic sources (DISS), version 3.2.0: A compilation of potential sources for earthquakes larger than M 5.5 in Italy and surrounding areas. *Istituto Nazionale di Geofisica e Vulcanologia*. <https://doi.org/10.6092/INGV.IT-DISS3.2.0>
- Fantoni, R. and Franciosi, R. (2010) Tectono-sedimentary setting of the Po Plain and Adriatic foreland. *Rendiconti. Lincei.*, **21**(S1), 197–209.
- Ferranti, L., Antonioli, F., Mauz, B., Amorosi, A., Dai Pra, G., Mastroruzzi, G., Monaco, C., Orrù, P., Pappalardo, M., Radtke, U., Renda, P., Romano, P., Sanso, P. and Verrubbi, V. (2006) Markers of the last interglacial sea-level high stand along the coast of Italy: tectonic implications. *Quat. Int.*, **145–146**, 30–54.
- Fielding, C.R., Ashworth, P.J., Best, J.L., Prokocki, E.W. and Sambrook Smith, G.H. (2012) Tributary, distributary and other fluvial patterns: What really represents the norm in the continental rock record? *Sed. Geol.*, **261–262**, 15–32.
- Fontana, A., Mozzi, P. and Marchetti, M. (2014) Alluvial fans and megafans along the southern side of the Alps. *Sediment. Geol.*, **301**, 150–171.
- Fontana, D., Amoroso, S., Minarelli, L. and Stefani, M. (2019) Sand liquefaction phenomena induced by a blast test: new insights from composition and texture of sands (late Quaternary, Emilia, Italy). *J. Sediment. Res.*, **89**(1), 13–27.
- Fontana, D., Lugli, S., Marchetti Dori, S., Caputo, R. and Stefani, M. (2015) Sedimentology and composition of sands injected during the seismic crisis of May 2012 (Emilia, Italy): clues for source layer identification and liquefaction regime. *Sediment. Geol.*, **325**, 158–167.
- Garver, J.I., Royce, P.R. and Smick, T.A. (1996) Chromium and nickel in shale of the Taconic foreland: a case study for the provenance of fine-grained sediments with an ultramafic source. *J. Sediment. Res.*, **66**, 100–106.

- Garzanti, E., Vezzoli, G. and Andò, S.** (2011) Paleogeographic and paleodrainage changes during Pleistocene glaciations (Po Plain, Northern Italy). *Earth Sci. Rev.*, **105**, 25–48.
- GeoMol Team** (2015) GeoMol, Assessing subsurface potentials of the Alpine Foreland Basins for sustainable planning and use of natural resources. Alpine Space Programme, Project Report, p. 188.
- Ghielmi, M., Minervini, M., Nini, C., Rogledi, S. and Rossi, M.** (2013) Late Miocene-Middle Pleistocene sequences in the Po Plain—Northern Adriatic Sea (Italy): The stratigraphic record of modification phases affecting a complex foreland basin. *Mar. Pet. Geol.*, **42**, 50–81.
- Gibling, M.R.** (2006) Width and thickness of fluvial channel bodies and valley fills in the geological record: a literature compilation and classification. *J. Sediment. Res.*, **76**, 731–770.
- Gibling, M.R., Tandon, S.K., Sinha, R. and Jain, M.** (2005) Discontinuity-bounded alluvial sequences of the southern Gangetic plains, India: aggradation and degradation in response to monsoonal strength. *J. Sediment. Res.*, **75**, 369–385.
- Gile, L.H., Hawley, J.W. and Grossman, R.B.** (1981) *Soils and Geomorphology in the Basin and Range Area of Southern New Mexico - Guidebook to the Desert Project*. New Mexico Bureau of Mines and Mineral Resources, Socorro, 222 pp.
- Govindaraju, K.** (1989) Compilation of working values and sample description for 272 geostandards. *Geostandards Newslett.*, **13**, 1–114.
- Green, A.N.** (2009) Palaeo-drainage, incised valley fills and transgressive systems tract sedimentation of the northern KwaZulu-Natal continental shelf, South Africa, SW Indian Ocean. *Mar. Geol.*, **263**, 46–63.
- Greggio, N., Giambastiani, B.M.S., Campo, B., Dinelli, E. and Amorosi, A.** (2018) Sediment composition, provenance and Holocene paleoenvironmental evolution of the Southern Po River coastal plain (Italy). *Geol. J.*, **53**, 914–928.
- Gunderson, K.L., Pazzaglia, F.J., Picotti, V., Anastasio, D.A., Kodama, K.P., Rittenou, R.T., Frankel, K.F., Ponza, A., Berti, C., Negri, A. and Sabbatini, A.** (2014) Unraveling tectonic and climatic controls on synorogenic growth strata (Northern Apennines, Italy). *GSA Bull.*, **126–3(4)**, 532–552.
- Hanneman, D.L. and Wideman, C.J.** (2006). Calcic pedocomplexes 2 Regional sequence boundary indicators in Tertiary deposits of the Great Plains and western United States. In: *Paleoenvironmental Record and Applications of Calcretes and Palustrine Carbonates* (Eds Alonso-Zarza, A.M. and Tanner, L.H.), *Geological Society of America Special Paper*, **46**, 1215.
- Hanneman, D.L. and Wideman, C.J.** (2010) Continental Sequence Stratigraphy and Continental Carbonates. In: van Loon A.J. (ed.), *Developments in Sedimentology*, 62, Carbonates. In: *Continental Settings: Geochemistry, Diagenesis and Applications* (Eds Alonso-Zarza, A.M. and Tanner, L.H.), pp. 215–273. Elsevier, Amsterdam.
- Kasse, C., Bohncke, S.J.P., Vandenberghe, J. and Gábris, G.** (2010) Fluvial style changes during the last glacial interglacial transition in the middle Tisza valley (Hungary). *Proc. Geol. Assoc.*, **121(2)**, 180–194.
- Kraus, M.J.** (1999) Paleosols in clastic sedimentary rocks: their geologic applications. *Earth Sci. Rev.*, **47**, 41–70.
- Kraus, M.J., Woody, D.T., Smith, J.J. and Dukicet, V.** (2015) Alluvial response to the Paleocene-Eocene Thermal Maximum climatic event, Polecat Bench, Wyoming (U.S.A.). *Palaeogeogr., Palaeoclimatol., Palaeoecol.*, **435**, 177–192.
- Kvale, E.P. and Archer, A.W.** (2007) Paleovalley fills: Trunk vs. tributary. *AAPG Bulletin*, **91(6)**, 809–821.
- Labourdette, R. and Jones, R.R.** (2007) Characterization of fluvial architectural elements using a three-dimensional outcrop data set: Escanilla braided system, southcentral Pyrenees, Spain. *Geosphere*, **3**, 422–434.
- Larson, P.H., Dorn, R.I., Faulkner, D.J. and Friend, D.A.** (2015) Toe-cut terraces: A review and proposed criteria to differentiate from traditional fluvial terraces. *Prog. Phys. Geogr.*, **39(4)**, 417–439.
- Leeder, M.R. and Stewart, M.D.** (1996) Fluvial incision and sequence stratigraphy: alluvial responses to relative sea-level fall and their detection in the geological record. In: *Sequence Stratigraphy in British Geology* (Eds Hesselbo, S.P. and Parkinson, D.N.), *Geological Society Special Publication*, **103**, 25–39.
- Leoni, L., Menichini, M. and Saitta, M.** (1986) Determination of S, Cl, and F in silicate rocks by X-ray fluorescence analyses. *X-Ray Spectrom.*, **11**, 156–158.
- Lewis, S.G., Maddy, D. and Scaife, R.G.** (2001) The fluvial system response to abrupt climate change during the last cold stage: the Upper Pleistocene River Thames fluvial succession at Ashton Keynes, UK. *Glob. Planet. Change*, **28**, 341–359.
- Lisiecki, L.E. and Raymo, M.E.** (2005) A Plio-Pleistocene stack of 57 globally distributed benthic $\delta^{18}\text{O}$ records. *Paleoceanography*, **20**. <https://doi.org/10.1029/2004PA001071PA1003>
- Livani, M., Scrocca, D., Arecco, P. and Doglioni, C.** (2018) Structural and stratigraphic control on salient and recess development along a thrust belt front: The Northern Apennines (Po Plain, Italy). *J. Geophys. Res. Solid Earth*, **123**, 4360–4387.
- Lugli, S., Marchetti Dori, S., Fontana, D. and Panini, F.** (2004) Composition of sands in cores along the high-speed rail (TAV): preliminary indications on the sedimentary evolution of the Modena plain. *Alpine Mediterran. Quatern.*, **17**, 379–389.
- Lugli, S., Marchetti Dori, S. and Fontana, D.** (2007). Alluvial sand composition as a tool to unravel the Late Quaternary sedimentation of the Modena plain, northern Italy. In: *Sedimentary Provenance and Petrogenesis: Perspectives from Petrography and Geochemistry* (Eds Arribas, J., Critelli, S., and Johnsson, M.J.). *Geological Society of America. Special Paper*, **420**, 57–72.
- Luzar-Oberiter, B., Mikes, T., von Eynatten, H. and Babic, L.** (2009) Ophiolitic detritus in Cretaceous clastic formations of the Dinarides (NW Croatia): evidence from Cr-spinel chemistry. *Int. J. Earth Sci.*, **98**, 1097–1108.
- Machette, M.N.** (1985) Calcic soils of the southwestern United States. *Geol. Soc. Am. Spec. Pap.*, **203**, 1–21.
- Mancini, M., Moscatelli, M., Stigliano, F., Cavinato, G.P., Milli, S., Pagliaroli, A., Simionato, M., Brancaloni, R., Cipolloni, I., Coen, G., Di Salvo, C., Garbin, F., Lanzo, G., Napoleoni, Q., Scarapazzi, M., Storoni Ridolfi, S. and Vallone, R.** (2013) The Upper Pleistocene-Holocene fluvial deposits of the Tiber River in Rome (Italy): lithofacies, geometries, stacking pattern and chronology. *J. Mediterranean Earth Sci.*, **5**, 95–101.
- Martelli, L., Bonini, M., Calabrese, L., Corti, G., Ercolessi, G., Molinari, F.C., Piccardi, L., Pondrelli, S., Sani, F. and Severi, P.** (2017) *Seismotectonic map of Emilia Romagna*

- Region and surrounding areas to scale 1:250,000. D.R.E.Am. MAP, Pistoia.
- Martinsen, O.J., Ryseth, A., Helland-Hansen, W., Flesche, H., Torkildsen, G. and Idil, S.** (1999) Stratigraphic base level and fluvial architecture: Ericson Sandstone (Campanian), Rock Springs Uplift, SW Wyoming, USA. *Sedimentology*, **46**, 235–259.
- McCarthy, P.J. and Plint, A.G.** (1998) Recognition of interfluvial sequence boundaries: integrating paleopedology and sequence stratigraphy. *Geology*, **26**, 3872390.
- McCarthy, P.J. and Plint, A.G.** (2013) A pedostratigraphic approach to nonmarine sequence stratigraphy: A three-dimensional paleosol-landscape model from the Cretaceous (Cenomanian) Dunvegan Formation, Alberta and British Columbia, Canada. In: *New Frontiers in Paleopedology and Terrestrial Paleoclimatology: Paleosols and Soil Surface Analog Systems* (Eds Driese, S.C., Nordt, L.C. and McCarthy, P.J.). *Society for Sedimentary Geology Special Publication*, **104**, 159–177.
- McCarthy, T.S., Tooth, S., Jacobs, Z., Rowberry, M.D., Thompson, M., Brandt, D., Hancox, P.J., Marren, P.H., Woodborne, S. and Ellery, W.N.** (2011) The origin and development of the Nyl River floodplain wetland, Limpopo Province, South Africa: trunk–tributary river interactions in a dryland setting. *S Afr Geogr J*, **93**, 172–190.
- Meade, R.H. and Moody, J.A.** (2010) Causes for the decline of suspended-sediment discharge in the Mississippi River system, 1940–2007. *Hydrol Process*, **24**, 35–49.
- Miall, A.D.** (1985) Architectural-element analysis: A new method of facies analysis applied to fluvial deposits. *Earth Sci Rev*, **22**, 261–308.
- Miall, A.D.** (1996) *The Geology of Fluvial Deposits: Sedimentary Facies, Basin Analysis, and Petroleum Geology*. Springer-Verlag, Berlin, 582 pp.
- Morton, R.A. and Suter, J.R.** (1996) Sequence stratigraphy and composition of late Quaternary shelf-margin deltas, northern Gulf of Mexico. *Am. Assoc. Petrol. Geol. Bull.*, **80**, 505–530.
- Muttoni, G., Carcano, C., Garzanti, E., Ghielmi, M., Piccin, A., Pini, R., Rogledi, S. and Sciunnach, D.** (2003) Onset of major Pleistocene glaciations in the Alps. *Geology*, **31**, 989–992.
- Muttoni, G., Scardia, G., Kent, D.V., Morsiani, E., Tremolada, F., Cremaschi, M. and Peretto, C.** (2011) First dated human occupation of Italy at ~0.85 Ma during the late Early Pleistocene climate transition. *Earth Planet Sci. Lett.*, **307**, 241–252.
- Newell, A.J., Sorensen, J.P.R., Chambers, J.E., Wilkinson, P.B., Uhlemann, S., Roberts, C., Gooddy, D.C., Vane, C.H. and Binley, A.** (2015) Fluvial response to Late Pleistocene and Holocene environmental change in a Thames chalkland headwater: the Lambourn of southern England. *Proc. Geol. Assoc.*, **126**, 683–697.
- Pellegrini, C., Asioli, A., Bohacs, K.M., Drexler, T.M., Feldman, H.R., Sweet, M.L., Maselli, V., Rovere, M., Gamberi, F., Valle, G.D. and Trincardi, F.** (2018) The late Pleistocene Po River lowstand wedge in the Adriatic Sea: Controls on architecture variability and sediment partitioning. *Mar. Pet. Geol.*, **96**, 16–50.
- Phillips, J.D.** (2011) Universal and local controls of avulsions in southeast Texas Rivers. *Geomorphology*, **130**, 17–28.
- Pondrelli, S., Salimbeni, S., Perfetti, P. and Danecsek, P.** (2012) Quick regional centroid moment tensor solutions for the Emilia 2012 (northern Italy) seismic sequence. *Ann. Geophys.*, **55**, 615–621.
- Posamentier, H.W.** (1998) Modifications of the sequence stratigraphic model with emphasis on passive margins (abs.). *AAPG Bulletin*, **82**, 1953.
- Posamentier, H.W.** (2001) Lowstand alluvial bypass systems: Incised vs. unincised. *AAPG Bulletin*, **85**(10), 1771–1793.
- Posamentier, H.W. and Allen, G.P.** (1999) Siliciclastic sequence stratigraphy: concepts and applications. *SEPM Concept Sedimentol. Paleontol.*, **9**, 210.
- Posamentier, H.W. and Vail, P.R.** (1988). Eustatic controls on clastic deposition, II. Sequence and systems tract models. In: *Sea-Level Changes: An Integrated Approach* (Eds Wilgus, C.K., Hastings, B.S., Kendall C.G.S.C., Posamentier, H.W., Ross, C.A. and Van Wagoner, J.C.), *Soc. Econ. Paleontol. Mineral., Spec. Publ.*, **42**, 125–154.
- Reimer, P., Austin, W., Bard, E., Bayliss, A., Blackwell, P., Bronk Ramsey, C., Butzin, M., Cheng, H., Edwards, R., Friedrich, M., Grootes, P., Guilderson, T., Hajdas, I., Heaton, T., Hogg, A., Hughen, K., Kromer, B., Manning, S., Muscheler, R., Palmer, J., Pearson, C., van der Plicht, J., Reimer, R., Richards, D., Scott, E., Southon, J., Turney, C., Wacker, L., Adolphi, F., Büntgen, U., Capano, M., Fahrni, S., Fogtmann-Schulz, A., Friedrich, R., Köhler, P., Kudsk, S., Miyake, F., Olsen, J., Reinig, F., Sakamoto, M., Sookdeo, A. and Talamo, S.** (2020) The IntCal20 Northern Hemisphere radiocarbon age calibration curve (0–55 cal kBP). *Radiocarbon*, **62**, 1–33.
- Remitti, F., Vannucchi, P., Bettelli, G., Fantoni, L., Panini, F. and Vescovi, P.** (2011) Tectonic and sedimentary evolution of the frontal part of an ancient subduction complex at the transition from accretion to erosion: The case of the Ligurian wedge of the northern Apennines, Italy. *Geol. Soc. Am. Bull.*, **123**(1–2), 51–70.
- Ricci Lucchi, F.** (1987) Semi-allochthonous sedimentation in the Apenninic thrust belt. *Sed. Geol.*, **50**, 119–134.
- Ricci Lucchi, F., Colalongo, M.L., Cremonini, G., Gasperi, G., Iaccarino, S., Papani, G., Raffi, S. and Rio, D.** (1982). Evoluzione sedimentaria e paleogeografica nel margine appenninico. In: *Guida Alla Geologia del Margine Appenninico-padano* (Eds Cremonini, G. and Ricci Lucchi, F.). *Guida Geol. Reg., Sot. Geol. Ital.*, 17–46.
- Richardson, J.L. and Vepraskas, M.J.** (2001). *Wetland Soilgenesis, Hydrology, Landscapes, and Classification*. CRC Press, LLC, Boca Raton, FL, 417 pp.
- Robertson, P.K., Campanella, R.G., Gillespie, R.G. and Greig, J.** (1986). Use of piezometer cone data. *Proc., In-situ '86, ASCE Specialty Conf.*, Blacksburg, VA.
- Scardia, G., Muttoni, G. and Sciunnach, D.** (2006) Subsurface magnetostratigraphy of Pleistocene sediments from the Po Plain (Italy): Constraints on rates of sedimentation and rock uplift. *Geol. Soc. Am. Bull.*, **118**, 1299–1312.
- Schmertmann, J.H.** (1969). Dutch friction-cone penetrometer exploration of a research area at Field 5, Eglin Air Force Base, Florida. U.S. Army Eng. Waterways Exp. Stat., Vicksburg, Miss., Contract Rep. S-69-4.
- Schumm, S.A.** (1993) River response to base level change-implications for sequence stratigraphy. *J. Geol.*, **101**(2), 279–294.
- Scognamiglio, L., Margheriti, L., Mele, F.M., Tinti, E., Bono, A., De Gori, P., Lauciani, V., Lucente, F.P., Mandiello, A.G., Marcocci, C., Mazza, S., Pintore, S. and Quintiliani, M.** (2012) The 2012 Pianura Padana Emiliana seismic sequence: locations, moment tensors and magnitudes. *Ann. Geophys.*, **55**, 549–559.

- Simms, A.R. and Rodriguez, A.B.** (2015) The influence of valley morphology on the rate of bayhead delta progradation. *J. Sediment Res.*, **2015**(85), 38–44.
- Singh, I.B.** (1972) On the bedding in the natural-levee and point-bar deposits of the Gomti River, Uttar Pradesh, India. *Sed. Geology*, **7**, 309–317.
- Singh, S.K., Rai, S.K. and Krishnaswami, S.** (2008) Sr and Nd isotopes in river sediments from the Ganga Basin: Sediment provenance and spatial variability in physical erosion. *J. Geophys. Res.*, **113**, F03006. <https://doi.org/10.1029/2007JF000909>.
- Sinha, R., Kettanah, Y., Gibling, M.r., Tandon, S.k., Jain, M., Bhattacharjee, P.s., Dasgupta, A.s. and Ghazanfari, P.** (2009) Craton-derived alluvium as a major sediment source in the Himalayan Foreland Basin of India. *GSA Bulletin*, **121**(11/12), 1596–1610.
- Soil Survey Staff** (1999) Soil taxonomy. A basic system of soil classification for making and interpreting soil surveys. In: *Agricultural Handbook*, 2nd edn. Natural Resources Conservation Service, USDA, Washington DC. 436 pp.
- Stolt, M.H. and Rabenhorst, M.C.** (2011). Introduction and historical development of subaqueous soil concepts. In: *Handbook of Soil Science* (Ed. Huang, P.M.), CRC Press, LLC, Boca Raton, FL. <https://www.routledgehandbooks.com/doi/10.1201/b11267-71>
- Stouthamer, E., Cohen, K.M. and Gouw, M.J.P.** (2011) Avulsion and its implications for fluvial-deltaic architecture: insights from the Holocene Rhine-Meuse delta. *SEPM Spec. Publ.*, **97**, 215–232.
- Tentori, D., Amorosi, A., Milli, S. and Marsaglia, K.M.** (2021) Sediment dispersal pathways in the Po coastal plain since the Last Glacial Maximum: Provenance signals of autogenic and eustatic forcing. *Basin Res.*, **33**, 1407–1428.
- Tentori, D., Marsaglia, K.M. and Milli, S.** (2016) Sand compositional changes as a support for sequence-Stratigraphic interpretation: The middle upper Pleistocene to Holocene deposits of the roman basin (Rome, Italy). *J. Sediment. Res.*, **86**(10), 1208–1227.
- Tentori, D., Milli, S. and Marsaglia, K.M.** (2018) A source-to-sink compositional model of a present highstand: An example in the low-rank Tiber depositional sequence (Latium tyrrhenian margin, Italy). *J. Sediment. Res.*, **88** (10), 1238–1259.
- Toscani, G., Burrato, P., Di Bucci, D., Seno, S. and Valensise, G.** (2009) Plio-Quaternary tectonic evolution of the Northern Apennines thrust fronts (Bologna-Ferrara section, Italy): seismotectonic implication. *Boll. Soc. Geol. Ital.*, **128–2**, 605–613.
- Turrini, C., Lacombe, O. and Roure, F.** (2014) Present-day 3D structural model of the Po Valley basin, Northern Italy. *Mar. Pet. Geol.*, **56**, 266–289.
- Vis, G.J., Kasse, C. and Vandenberghe, J.** (2008) Late Pleistocene and Holocene palaeogeography of the Lower Tagus Valley (Portugal): effects of relative sea level, valley morphology and sediment supply. *Quatern. Sci. Rev.*, **27**, 1682–1709.
- Vittori, E. and Ventura, G.** (1995) Grain size of fluvial deposits and late Quaternary climate: A case study in the Po River valley (Italy). *Geology*, **23**(8), 735–738.
- Waelbroeck, C., Labeyrie, L., Michel, E., Duplessy, J.C., McManus, J.F., Lambeck, K., Balbon, E. and Labracherie, M.** (2002) Sea-level and deep water temperature changes derived from benthic foraminifera isotopic records. *Quatern. Sci. Rev.*, **21**(1–3), 295–305.
- Wright, V.P. and Marriott, S.B.** (1993) The sequence stratigraphy of fluvial depositional systems: The role of floodplain sediment storage. *Sed. Geol.*, **86**, 203–210.
- Xu, J.** (2016) Sediment jamming of a trunk stream by hyperconcentrated floods from small tributaries: case of the Upper Yellow River, China. *Hydrolog. Sci. J.*, **61**(10), 1926–1940.
- Zuffa, G.G.** (1985) Optical analyses of arenites: influence of methodology on compositional results. In: *Provenance of Arenites* (Ed. Zuffa, G.), pp. 165–189. D. Reidel, NATO Advanced Study Institute, Dordrecht.

Manuscript received 25 August 2020; revision accepted 3 April 2021

Supporting Information

Additional information may be found in the online version of this article:

Data S1. List of radiocarbon dates used in this work.